

Sex-specific maladaptive responses to acute stress

upon in utero THC exposure are mediated by dopamine

1
2
3
4
5
6
7
8
9
10
11
12
13
14
15
16
17
18
19
20
21
22
23
24
25
26
27
28
29
30
31
32
33
34
35
36
37
38
39
40
41
42
43
44
45
46
47
48
49
50
51
52
53
54
55
56
57
58
59
60
61
62
63
64
65

Serra Valeria¹, Traccis Francesco¹, Aroni Sonia¹, Vidal Palencia Laura², Concas Luca¹, Serra
Marcello¹, Leone Roberta¹, Porcu Patrizia³, Busquets Garcia Arnau², Frau Roberto¹, Melis Miriam¹

¹Dept. Biomedical Sciences, Div. Neuroscience and Clinical Pharmacology, University of Cagliari,
Italy; ²Hospital del Mar Research Institute, Barcelona, Spain; ³Institute of Neurosciences, National
Research Council (C.N.R.), Cagliari, Italy.

Corresponding author:

Miriam Melis, PhD

Department of Biomedical Sciences

Division of Neuroscience and Clinical Pharmacology

Cittadella Universitaria di Monserrato

09042 Monserrato (CA)

Italy

tel: +39 070 675 4322

fax: +39 070 675 4320

email: myriam@unica.it

Abstract

1
2
3 Cannabis remains by far the most consumed illicit drug in Europe. The availability of more potent
4 cannabis has raised concerns regarding the enhanced health risks associated with its use,
5 particularly among pregnant women. Growing evidence shows that cannabis use during
6 pregnancy increases the risks of child psychopathology. We have previously shown that **only**
7 male rat offspring prenatally exposed to Δ^9 -tetrahydrocannabinol (THC), a rat model of prenatal
8 cannabinoid exposure (PCE), display a hyperdopaminergic phenotype associated with a
9 differential susceptibility to acute THC- and stress-mediated effects on sensorimotor gating
10 functions. Here, we explore the contribution of the hypothalamic-pituitary-adrenal (HPA) axis, key
11 regulator of body adaptive stress responses, to the detrimental effects of acute stress on ventral
12 tegmental area (VTA) dopamine neurons and sensorimotor gating function of PCE rats. We
13 report a sex-dependent compromised balance in mRNA levels of genes encoding
14 mineralocorticoid and glucocorticoid receptors in the VTA, alongside with stress-induced pre-
15 pulse inhibition (PPI) **impairment**. Notably, VTA dopamine neuronal activity is causally linked to
16 the manifestation of stress-dependent deterioration of PPI. Finally, pharmacological
17 manipulations targeting glycogen-synthase-kinase-3- β signaling during postnatal development
18 correct these stress-induced, sex-specific and dopamine-dependent **disruption** of PPI.
19 Collectively, these results highlight the critical sex-dependent interplay between HPA axis and
20 dopamine system in the regulation of sensorimotor gating functions in rats.
21
22
23
24
25
26
27
28
29
30
31
32
33
34
35
36
37
38
39
40
41
42
43
44
45
46
47

48 **Keywords:** Cannabis; Dopamine; DREADD; HPA axis; Neurodevelopment; Psychopathology;
49 Stress; Vulnerability
50
51
52
53
54
55
56
57
58
59
60
61
62
63
64
65

1. Introduction

Mental disorders affect 25% of the population worldwide and more than one-third of these are established by 14.5 years of age [1-3]. Stress is widely accepted as a detrimental factor for mental wellbeing, leading the World Health Organization to classify it as the “health epidemic of the 21st century” [4], with stress-related mental illnesses progressively increasing worldwide, particularly in youth [5]. However, it is still unclear why some individuals are more susceptible to developing stress-induced psychopathology, while others are more resilient and/or recover more rapidly [6, 7].

Many factors regulate our ability to cope with stress, including inter-individual differences due to genetic background, gender/sex, and early life adversities. Adaptive responses to stress can be modified by experience, which can increase the sensitivity of the hypothalamic-pituitary-adrenal (HPA) axis and dopamine system and produce inadequate stress reactions [8, 9]. When adverse experiences occur early in life, they might impact on developmental trajectory of different systems and circuitries with long-lasting and profound effects [7, 10, 11]. A functional interplay between the HPA axis and dopamine system plays an important role for adequate coping strategies in reaction to stressful conditions [8, 9, 12, 13]. Preclinical studies have demonstrated that acute stressors activate dopamine neurons [14] promoting long-lasting neuroplastic changes [15, 16] and leading to a gain-of-function of dopamine signaling that might alter the individual coping strategies to subsequent insults later in life [13]. Acute stress is also associated with mesolimbic dopamine release in humans [17]. Understanding how early life adversities contribute to both vulnerability to and resilience against acute stress and manifestation of psychopathology is crucial to implement early diagnosis and treatment, and to improve clinical outcome [7, 18].

Clinical evidence shows that among early life adversities prenatal cannabis exposure (PCE) is a predictive risk factor for the development of offspring psychopathology [19-26], and is associated with alterations in cortisol levels [27-29]. However, cannabis use during pregnancy has been on an alarming sharp rise [30, 31], with the greatest use during the first trimester [32]. Indeed, cannabis increasing legal availability is most likely leading to the common misconception that it is a safe natural remedy to be used even during pregnancy [33-35]. We have previously found that, in a rat model of

1 PCE, male but not female subjects manifest an at-risk psychopathological endophenotype for a
2 quantifiable trait of **deterioration** in sensorimotor gating functions upon a single exposure to the
3 cannabis main psychoactive ingredient, delta9-tetrahydrocannabinol (THC) [36]. This is associated
4 with a sex-specific mesolimbic hyperdopaminergia [36, 37], a hallmark of disrupted sensorimotor
5 gating functions [38-41]. We also found that pre-pulse inhibition (PPI) of the startle reflex [42, 43], a
6 cross-species validated operational measure of sensorimotor gating functions, was impaired in PCE
7 males upon either an otherwise ineffective dose of dopamine receptor agonist apomorphine or an
8 acute stressor [44]. Of note, sex-specific failure in adopting coping strategies in response to an acute
9 unescapable stressor were manifest as a consequence of PCE [37, 44].

10
11 In this study, we investigated how sex contributes to a PCE-induced vulnerability to the effects of
12 acute stress. By using behavioral and molecular analyses, we found that **PCE progeny exhibit male-**
13 **specific exaggerated responses to an acute inescapable stressor**. By using chemogenetic
14 approaches, we showed the causal role of dopamine neuron activity of the ventral tegmental area
15 (VTA) in the deteriorating effects of acute inescapable stressors on sensorimotor gating functions.
16 Finally, such maladaptive stress responses in PCE males could be prevented by postnatal treatment
17 with either pregnenolone or lithium, two inhibitors of glycogen synthase kinase-3 beta (GSK-3 β)
18 signaling pathway. Our data expand our understanding of the sex-specific impact of PCE on
19 dopamine neurodevelopmental trajectories suggesting molecular targets for therapeutic intervention
20 of offspring exposed to cannabis during pregnancy and suggest a causal link between a
21 hyperdopaminergic profile and stress-induced **disruption** of PPI.

2. Materials and Methods

2.1 Subjects

22 All experimental procedures were performed in accordance with the European legislation EU
23 Directive 2010/63 and were approved by the Animal Ethics Committees of the University of Cagliari

and by the Italian Ministry of Health (Authorization n° 256/2020). We made all efforts to minimize pain and suffering and to reduce the number of animals.

2.2 Drugs and treatments

2.2.1 Drugs and chemicals

THC resin was purchased from THC PHARM GmbH (Frankfurt, Germany) and dissolved in ethanol at 20 % final concentration. THC was diluted with sterile saline (0.9 % NaCl) containing 1-2 % Tween® 80. Clozapine-N-oxide dihydrochloride (CNO, Tocris Bioscience) was dissolved in sterile saline (0.9% NaCl). CNO was administered intra-peritoneally (i.p.) at 2 ml per kg body weight, 30 minutes prior to **pre-pulse inhibition (PPI)** test. Pregnenolone (PREG, Sigma-Aldrich) and lithium were administered subcutaneously (s.c.) at 2 ml per kg body weight once per day from gestational day (GD) 15 to post-natal day (PND) 23. PREG and lithium (Sigma-Aldrich) were dissolved in 20 % β -Cyclodextrin and sterile saline (0.9 % NaCl), respectively.

2.2.2 Treatments

Primiparous female Sprague Dawley rats (Envigo) were used as mothers and single housed during pregnancy. Sprague Dawley dams expressing Cre recombinase under the control of the *TH* promoter (*TH::Cre*) were used for the DREADD experiments. THC or vehicle was administered (2 mg per kg, 1 ml per kg, s.c. once per day) from GD5 to GD20. This dose of THC was chosen because it does not produce behavioral responses or cannabinoid tolerance after repeated administration [45]. Moreover, this dose does not have any substantial impact on maternal and non-maternal behavior, (5%) [46], **it achieves plasma concentrations in rodents (8.6-12.4 ng/ml) comparable to human recreational cannabis smokers consuming cannabis derivatives with a 7% THC (13-63 ng/ml, 0–22h post-inhalation) [47, 48] and in aborted fetal tissues of pregnant cannabis users (4-287 ng/mL) [49].** **The progeny was** weaned at PND 21 and were housed in a climate-controlled animal room (21 ± 1 °C; 60 % humidity) under a normal 12 h light-dark cycle (lights on at 7:00 a.m.) with *ad libitum* access to water and food until the experimental day (PND25-28). To control for litters effects, we did not use more than two offsprings from each litter for the same experiment.

1
2
3
4
5
6
7
8
9
10
11
12
13
14
15
16
17
18
19
20
21
22
23
24
25
26
27
28
29
30
31
32
33
34
35
36
37
38
39
40
41
42
43
44
45
46
47
48
49
50
51
52
53
54
55
56
57
58
59
60
61
62
63
64
65

2.3 Surgical procedures

For chemogenetic manipulation, *TH::Cre*-positive offspring were stereotaxically bilaterally injected under isoflurane (4-5 % induction, 1-2 % maintenance) with a Cre-dependent adeno-associated virus expressing an inhibitory or excitatory DREADD construct, AAV5-hSyn-DIO-hM4D(Gi)-mCherry and AAV5-hSyn-DIO-hM3D(Gq)-mCherry, respectively, or control virus (AAV5-hSyn-DIO-mCherry) to target dopaminergic neurons in the VTA at PND7 (-4.2 mm posterior to bregma, ± 0.55 mm lateral to bregma, -5.25 mm ventral from the cortical surface) with a Hamilton syringe. Viruses were injected at a volume of 0.5 μ l per side at a rate of 0.1 μ l/min. Injection needles were left in place for 5 min after the injection to ensure adequate viral delivery. For all the experiments the virus was incubated for at least 21 days, when expression was identifiable by the reporter protein expression.

2.4 Behavioral experiments

2.4.1 Forced swim test and acute restraint stress

The forced swim test (FST) was conducted as previously described [44]. Briefly, rats were placed for 10 min in a transparent cylinder (40 cm high \times 20 cm in diameter) filled with cold water to a depth of 30 cm, ensuring that the animals were unable to stabilize themselves by touching the bottom of the cylinder with their tails. After the FST, the rats were immediately dried out and then transferred to the startle cages for pre-pulse inhibition (PPI) testing.

Acute restraint stress (RS) was produced by placing the rat for 20 min in a well-ventilated, plastic tube (3.5 cm long \times 6 cm in diameter) with an adjustable end to accommodate the size of each animal, as previously described [44]. As with the FST, after the RS, the animals were immediately subjected to the PPI procedure.

2.4.2 Pre-pulse Inhibition test

1
2
3
4
5
6
7
8
9
10
11
12
13
14
15
16
17
18
19
20
21
22
23
24
25
26
27
28
29
30
31
32
33
34
35
36
37
38
39
40
41
42
43
44
45
46
47
48
Pre-pulse Inhibition (PPI) was tested following the protocol previously described [36]. The apparatus used to detect startle reflex and PPI parameters (Med Associates) consisted of four standard cages placed in sound-attenuated chambers with fan ventilation. Each cage consisted of a Plexiglas cylinder of 5 cm diameter, mounted on a piezoelectric accelerometric platform connected to an analog-digital converter. Two separate speakers conveyed background noise and acoustic bursts; each one properly placed so as to produce a variation of sound within 1 dB across the startle cage. On the testing day, each rat was placed in the cage for a 5-min acclimatization period consisting of 70-dB white noise background, which continued for the remainder of the session. Each session consisted of three consecutive sequences of trials (blocks). During the first and third blocks, rats were presented with only five pulse-alone trials of 115-dB. The second block consisted of a pseudorandom sequence of fifty trials, including twelve pulse-alone trials; thirty trials with a pulse preceded by 74-, 78-, or 82-dB prepulses (10 for each level of prepulse loudness); and eight no-stimulus trials, where only the background noise was delivered. Pulse and prepulse durations were set at 40 and 20 ms, respectively. Inter-trial intervals were selected randomly between 10 and 15 s, while the inter-stimulus intervals were set at 100 ms. The startle response was based on the first positive wave that meets the minimum wave criteria and determined as the mean startle amplitude of the pulse-alone trials relative to the second block. The % PPI was calculated only on the values relative to the second block using the following formula: $[(\text{mean startle amplitude for pulse alone trials} - \text{mean startle amplitude for prepulse + pulse trials}) / \text{mean startle amplitude for pulse alone trials}] \times 100$. Depending on the experimental procedures, the PPI test was conducted either immediately after stress or 30 min after systemic administration of CNO to ensure the engagement of Gq/Gi-DREADDs in the VTA.

49 50 51 52 53 54 55 56 57 58 59 60 61 62 63 64 65 **2.5 Immunohistochemistry and cell counting**

2.5.1 Tissue preparation

Following the behavioral experiments, rats at PND 26-34 were deeply anaesthetized with isoflurane and transcardially perfused with saline, followed by 4% paraformaldehyde in 0.1 M phosphate buffer (PB; pH=7.4). Afterwards, brains were removed, postfixed 2 h in the same solution at 4°C, then

1
2
3
4
5
6
7
8
9
10
11
12
13
14
15
16
17
18
19
20
21
22
23
24
25
26
27
28
29
30
31
32
33
34
35
36
37
38
39
40
41
42
43
44
45
46
47
48
49
50
51
52
53
54
55
56
57
58
59
60
61
62
63
64
65

rinsed three times in PB saline 1× (PBS) and preserved in the same solution at 4°C. The next day, brains were coronally cut on a vibratome (VT1000S, Leica Biosystems) to yield sections (thickness, 40 µm) suited for immunohistochemistry (IHC) processing. For each rat, three coronal sections representative of the VTA were collected based on stereotaxic coordinates ranging from -4.80 mm to -5.80 mm relative to bregma. These coordinates were referenced from the rat brain atlas by Paxinos and Watson [50].

2.5.2 Reaction protocol, image acquisition, and cell counting

Free-floating sections were rinsed in 0.1 M PB, blocked in a solution containing 10% normal goat serum (NGS, Vector, UK) and 0.5% Triton X-100 in 0.1 M PB at room temperature (2 h). Thereafter, sections were incubated at 4°C (48h) with the rabbit polyclonal primary antibody anti-TH (1:1000, Merck, Germany, #AB152), rinsed three times in 0.1 M PB, and then incubated with the secondary antibody, Atto® 488-labeled goat anti-rabbit IgG (1:400, Merck, Germany, #18772) in 0.1 M PB at room temperature (3 h). Afterward, sections were incubated for 10 minutes in 4',6-diamidino-2-phenylindole (DAPI; 1:10,000, Merck, Italy, D9542), to allow visualization of cell nuclei, rinsed in PB 0.1 M, and mounted onto super-frost glass slides using Mowiol® mounting medium.

Images of single wavelength (14-bit depth) were obtained with a ZEISS Axio Scan Z1 slide scanner (Zeiss, Germany). Brain sections were captured at 20× magnification (Objective: Plan-Apochromat 20×/0.8 M27) to acquire the whole VTA from both hemispheres. The ImageJ software (National Institutes of Health, USA) was used to quantify the number of TH+, mCherry+, and TH+-mCherry+ cells located in the VTA. Specifically, images were first background-adjusted, then cells were manually counted within the VTA by using the multi-point tool. Analyses were performed blind with respect to the treatment received by each animal. No significant differences in the relative proportion of TH+, mCherry+, and TH+-mCherry+ cells were found among the three sections, therefore values from different antero-posterior levels were averaged. For each experimental condition, the final percentages were calculated as an average of the values from each rat within the same experimental group.

2.6 Corticosterone and Adrenocorticotrophic hormone Analysis

1
2
3 Rats were sacrificed by decapitation and blood was immediately collected from the trunk into K3-
4 EDTA tubes, then centrifuged at 900×g for 15 min at 4°C; the resulting plasma was collected and
5 frozen at -20°C until assayed. An enzyme-linked immunosorbent assay (ELISA) was used to quantify
6
7 plasma levels of Corticosterone (CORT; #RE52211 IBL Corticosterone Enzyme Immunoassay Kit,
8
9 TECAN Europe), and Adrenocorticotrophic hormone (ACTH; #EK-001-21, Phoenix Pharmaceuticals
10
11 Inc., Burlingame, CA, USA), as previously described [51]. ELISA assays were performed according
12
13 to the manufacturer's instructions using a 96-well plate pre-coated with polyclonal antibodies against
14
15 an antigenic site on the CORT or ACTH molecules, respectively. The kits also provided a seven-
16
17 point standard curve ready to use (0 to 83.2 ng/ml, CORT) or a peptide standard for a six-point serial
18
19 dilutions (0 to 25 ng/ml, ACTH), as well as quality controls. Each sample was run in duplicate. CORT
20
21 and ACTH plasma levels are expressed in ng/ml. With regard to the stressed group, blood was
22
23 collected 30 min after the beginning of the forced swimming test (FST).
24
25
26
27
28
29

2.7 Quantitative Real-Time PCR Analysis

30
31
32 To characterize the gene expression levels of MRs and GRs, unstressed and stressed animals were
33
34 sacrificed by decapitation. The unstressed group is made up of naïve animals. Decapitation in
35
36 stressed animals was carried out after 30 min from the beginning of the forced swimming test (FST).
37
38
39

40 The brain was rapidly removed, and bilateral VTA tissue punches were manually dissected and
41
42 stored at -80°C until use. VTA samples were homogenized in a Douncer containing 1 mL of QIAzol
43
44 Lysis Reagent and then mixed with 200 μ L of chloroform. After centrifugation, the supernatant
45
46 (aqueous phase) was transferred to a new tube, and the RNeasy Lipid Tissue Mini Kit (QIAGEN)
47
48 was used according to the manufacturer's instructions. Once the total RNA was isolated, the quality
49
50 and concentration were assessed using a NanoDrop 1000 Spectrophotometer (Thermo Fisher
51
52 Scientific) and immediately stored at -80°C until further use. Total RNA from each VTA sample was
53
54 transcribed into complementary DNA (cDNA) using the High-Capacity cDNA Reverse Transcription
55
56 Kit (Applied Biosystems, CA, United States) in a 20- μ L reaction volume and stored at -20°C until
57
58 use. Reverse transcriptase reactions were conducted at 25°C for 10 min, 2 h at 37°C, and 5 min at
59
60
61
62
63
64
65

1
2
3
4
5
6
7
8
9
10
11
12
13
14
15
16
17
18
19
20
21
22
23
24
25
26
27
28
29
30
31
32
33
34
35
36
37
38
39
40
41
42
43
44
45
46
47
48
49
50
51
52
53
54
55
56
57
58
59
60
61
62
63
64
65

85°C. The final cDNA concentration was normalized across samples to 30 ng/μL with autoclaved Milli-Q water.

The MRs and GRs were assessed by qRT-PCR analyzing the gene expression levels of the nuclear receptor subfamily 3, group C, member 2 (*Nr3c2*) and the nuclear receptor subfamily 3, group C, member 1 (*Nr3c1*), respectively. Primers were designed and verified using the primer-BLAST design tool (Table 1). All samples were tested in triplicate and β-actin (*Actb* gene) was used as an endogenous housekeeping gene to normalize the transcriptional levels of all target genes analyzed. qRT-PCR was performed in an Optical 384-well plate with a QuantStudio™ 12K Sequence Detection System (Applied Biosystems, CA, United States) consisting of 2 activation steps (50°C for 2 min, then 95°C for 10 min) followed by 45 cycles of melting (95°C for 15 s) and annealing (60 °C for 1 min). The PCR reaction contained PowerUp SYBR Green Master Mix (Applied Biosystems, CA, United States). The comparative cycle threshold ($\Delta\Delta C_t$) method was used to establish the gene expression relative quantification (RQ), and the results were reported as fold change compared with the control (CTRL) group for each sex.

Table 1. Primers for MRs and GRs characterization

Gene	Forward primer (5'-3')	Reverse primer (5'-3')	Lenght	Reference
<i>Nr3c2</i>	GCCCGGCAAATCTCAACA ACT CAA	TTAGGGAAAGGAACGTCGTGAG CA	235	NM_001395 077.1
<i>Nr3c1</i>	GAAAAGCCATCGTCAA AAGGG	TGGAAGCAGTAGGTAAGGAGA	121	XM_039096 567.1
<i>Actb</i>	ACCCGCGAGTACAACCTTCT	ATGGCTACGTACATGGCTGG	470	XM_039089 807.1

2.8 Statistical analysis

Rats were randomly assigned to each group. Statistical analysis was performed with GraphPad Prism 8 (San Diego CA, USA). Data were analyzed using 2- or 3-way ANOVA when appropriated,

1 followed by Sidak's or Tukey's test. Significance threshold was set at $p < 0.05$. Data are presented
2 as means \pm SEM.
3
4
5
6

7 **3 Results**

8 **3.1 Acute stress does not impair gating functions in PCE female progeny**

9
10
11 Stress is one of the major determinants in the onset of dopamine-related psychopathologies [7, 8]
12 and sex differences in stress-coping strategies have been already reported in experimental animals
13 [7]. We previously found that PCE interferes with behavioral adaptations to an acute inescapable
14 stress, such as the forced swim test (FST), in male [44] but not in female offspring [37]. FST also
15 impairs subsequent PPI performance in PCE males [44]. To test whether PCE female rats were also
16 protected by the effects of this acute inescapable stressor (i.e., FST) on PPI, PCE rats were
17 subjected to FST before the PPI (Fig. 1A). FST induced sex-specific **disruption** in PPI, being CTRL
18 females less performant than males (Fig. 1B; 2way ANOVA, $F_{1,43} = 5.21$; $p = 0.0035$). Of note, FST
19 exerted sex-dependent PPI effects as a function of PCE (Fig. 1B; sex x PCE: 2way ANOVA, $F_{1,43} =$
20 14.35 ; $p = 0.0005$), supporting that PCE acts as a "first hit" [53] and endows the male offspring with
21 an aberrant salient attribution [44], whereas the females display a normal behavioral performance
22 [36, 37, 44]. To assess whether this reaction depends on a sex-specific engagement of the HPA axis
23 in the PCE progeny, we measured baseline and stress-induced rise of endogenous plasma
24 corticosterone (CORT) and adrenocorticotrophic hormone (ACTH) levels. First, in a cohort of
25 unstressed PCE rats, we verified whether PCE alters baseline CORT and ACTH levels as a function
26 of sex (Fig. 1A, C-D). No differences were found among the groups (CORT: stress x PCE x sex:
27 3way ANOVA, $F_{1,60} = 0.12$; $p = 0.7303$; ACTH: stress x PCE x sex: 3way ANOVA, $F_{1,60} = 2.01$; $p = 0.1613$;
28 Fig. 1C-D). Then, in line with previous findings [54], FST raised plasma CORT and ACTH
29 concentrations to a larger extent in female rats irrespective of PCE (CORT: 2way ANOVA,
30 $F_{1,32} = 15.28$; $p = 0.0005$; ACTH: 2way ANOVA, $F_{1,32} = 7.22$; $p = 0.0113$, Fig.1C-D). This suggests that
31 plasma CORT and ACTH levels neither drive sex-specific coping strategies to FST [37, 44] nor
32 stress-induced **impairments** in PPI progeny (Fig.1B and [44]).
33
34
35
36
37
38
39
40
41
42
43
44
45
46
47
48
49
50
51
52
53
54
55
56
57
58
59
60
61
62
63
64
65

3.2 Sex-specific modulation of HPA-axis response following acute stress

Under stress conditions, CORT acts by activating high-affinity mineralocorticoid receptors (MRs) and low-affinity glucocorticoid receptors (GRs). Particularly, CORT controls coping with and adaptation to changes through a receptor-mediated on- (MR) and off- (GR) switch, which needs to be in balance for providing the energy in maintaining homeostasis and health [7, 52, 55]. MR/GR imbalance is suggested to compromise HPA axis responses to stress [7, 52], where MR activation affects the peak rather than the duration of HPA-axis activity, which is under negative feedback control of GRs [52, 55]. Of note, CORT also acts locally in the VTA to modulate dopamine signaling [16, 56, 57]. To assess whether PCE induced an imbalance between MR- and GR- mediated actions, we determined mRNA levels of MR (*Nr3c2*) and GR (*Nr3c1*) in the VTA of preadolescent unstressed (naïve) and stressed rats by quantitative real-time PCR (Fig 2A). Key differences were found with a specific unbalance between mRNA levels of *Nr3c2* (2way ANOVA, $F_{1,33}=7.20$; $p=0.0113$; Fig.2B) and *Nr3c1* (2way ANOVA, $F_{1,44}=8.55$; $p=0.0054$; Fig.2C) as a function of PCE only in unstressed male rats. FST further decreased mRNA levels of *Nr3c1* in PCE males (2way ANOVA, $F_{1,44}=4.12$; $p=0.04$; Fig.2C), whereas it increased mRNA levels of *Nr3c2* in PCE females (*Nr3c2*: 2way ANOVA, $F_{1,25}=4.57$; $p=0.0425$; *Nr3c1*: 2way ANOVA, $F_{1,29}=2.12$; $p=0.1558$; Fig.2D-E), without modifying mRNA levels of *Nr3c2* (2way ANOVA, $F_{1,33}=0.01$; $p=0.89$; Fig.2B) in PCE males and *Nr3c1* (2way ANOVA, $F_{1,44}=0.01$; $p=0.91$; Fig. 2E) in females. Since MRs operate as an on-switch to select an appropriate coping response, whereas GRs serve as the off-switch to terminate the duration of the HPA-mediated reaction [7, 55], collectively, this data suggests that male-specific MR/GR imbalances might accompany an inadequate HPA axis reaction to FST [44] and might explain the subsequent impaired PPI (Fig. 1B and [44]).

3.3 Maladaptive responses to acute stress are mediated by dopamine

Dopamine role in the regulation of PPI has long been recognized [58-64] within an extremely complex circuit [41, 65]. However, the causative role of mesolimbic hyperdopaminergia underlying PPI disruption has never been tested by spatially isolating this single neural component. Given that PCE males exclusively exhibit a hyperdopaminergic phenotype [36], we tested the hypothesis that

1 stress-induced impairment of PPI in PCE males requires enhanced VTA dopamine signaling. We,
2 therefore, inhibited VTA dopamine cell activity before FST. To this aim, we induced the expression of
3
4 Gi-coupled hM4D receptor in VTA dopamine neurons by injecting a Cre-dependent adeno-
5 associated viral (AAV) vector, AAV5-hSyn-DIO-hM4D(Gi)-mCherry, into the VTA of male *TH::Cre*
6 transgenic rats (Fig. 3A) in which Cre mimics the expression of the rate-limiting enzyme for dopamine
7 synthesis, i.e., tyrosine hydroxylase (TH) [66]. Control rats received the AAV5-hSyn-DIO-mCherry
8 vector, which carried the gene for mCherry alone. Within the VTA of PCE males, 64.7±6.1 % of
9 mCherry labelled cells were also TH-positive, whereas only 35.3±6.1 % of transduced cells were TH-
10 negative. Similar results were obtained in CTRL males, where 63.4±13.8 % of mCherry-Gi labelled
11 cells were also TH-positive, while only 36.6±13.8 % of transduced cells were TH-negative (Fig. 3B),
12 confirming the cell specificity of the DREADD (designer receptors exclusively activated by designer
13 drugs) approach as previously described [67, 68]. Male rats were administered with clozapine N-
14 oxide (CNO, 3 mg/kg, i.p.) to inhibit VTA dopamine cells [67] before FST (Fig. 3C-D). Decreasing
15 VTA dopamine neuron activity did not affect the startle amplitude (Fig. 3C; 2way ANOVA Gi-
16 DREADD: $F_{1,78} = 0.34$; $p=0.56$), while it prevented FST-induced reduction of PPI in PCE male
17 offspring (Fig. 3D; 2way ANOVA Gi-DREADD: $F_{1,35} = 0.35$; $p=0.56$; 2way ANOVA Gi-DREADD x
18 PCE: $F_{1,24} = 11.7$; $p= 0.002$ and [44]). In addition, inhibiting VTA dopamine signaling via
19 chemogenetics prevented detrimental effects on PPI of another unavoidable stress condition, i.e.
20 acute restraint stress (RS) in PCE male rats (Fig. 3F; 2way ANOVA Gi-DREADD: $F_{1,21} = 0.035$;
21 $p=0.85$) (2way ANOVA PCE: $F_{1,34} = 6.17$; $p= 0.018$; Fig. 3F) without affecting the startle amplitude
22 (2way ANOVA Gi-DREADD: $F_{1,36} = 4.427e-006$, $p=0.99$; Fig. 3E). CNO is converted in clozapine
23 and, therefore, may have off-target effects at other endogenous receptors rather than at Gi-
24 DREADDs [69]. However, CNO administration in *TH::Cre* rats expressing a control fluorophore had
25 no effect on both startle amplitude and PPI performance (Fig. 3C-F), thus indicating that the
26 protective effects on PPI are DREADD-mediated and require normalizing VTA dopamine neuron
27 activity.

28 To examine the pathological role of a hyperdopaminergic phenotype in PPI regulation by acute
29 stress, we chemogenetically excited VTA DA cells [67] before FST in female rats, as female PPI

1 performance is not impacted by this acute unescapable stressor as a function of PCE (Fig. 1B). Of
2 note, PCE does not affect mesolimbic dopamine system function in female rats [37] and their PPI
3 performance is not affected by an acute challenge with THC [36]. We induced the expression of Gq-
4 coupled hM3D receptor in VTA dopamine neurons by injecting a Cre-dependent AAV vector, AAV5-
5 hSyn-DIO-hM3D(Gq)-mCherry, into the VTA of female TH::Cre transgenic rats (Fig. 4A). Control rats
6 received the AAV5-hSyn-DIO-mCherry vector, which carried the gene for mCherry alone. Within the
7 VTA of PCE females, 70.8±9.7 % of mCherry-Gq labelled cells were also TH-positive, whereas only
8 29.2±9.8 % of transduced cells were TH-negative. Similar results were obtained in CTRL females,
9 where 78.13±9.9 % of mCherry-Gq labelled cells were also TH-positive, while only 21.9±9.9 % of
10 transduced cells were TH-negative (Fig. 4B), in agreement with previous studies [70, 71]. Female
11 rats were administered with CNO to stimulate VTA dopamine cells before either FST and PPI (Fig.
12 4C). Importantly, a wide range of CNO doses, including 3 mg/kg, does not affect locomotor activity
13 of this TH::Cre transgenic rat [71] but see [72]. Unlike Gi-DREADD activation in males, in vivo
14 excitation of VTA dopamine neuron activity by CNO markedly reduced startle amplitude in both CTRL
15 and PCE females. This effect was observed after exposing animals to either FST or RS experimental
16 procedures (Fig. 4C; FST: 2way ANOVA, Gq-DREADD, $F_{1,66} = 5.71$, $p < 0.05$; Fig. 4D; RS: 2way
17 ANOVA, Gq-DREADD, $F_{1,61} = 65.89$; $p < 0.0001$). Importantly, no specific interactions among factors
18 were detected (FST: 2way ANOVA, interaction Gq-DREADD x PCE, $F_{1,66} = 2.88$, $p = 0.09$, Fig. 4D;
19 RS: 2way ANOVA, interaction Gq-DREADD x PCE, $F_{1,61} = 1.044$; $p = 0.31$, Fig. 4C), indicating that
20 PCE did not significantly affect the decrement in startle amplitude produced by Gq-DREADD
21 manipulation under both experimental stress conditions. Given that PPI data are extrapolated by
22 startle values, and Gq-DREADD stimulation elicited a robust reduction in startle magnitude in both
23 CTRL and PCE females, we reasoned to compute the percentage PPI to delta PPI in order to avoid
24 potential artifacts in data interpretation caused by "floor effects" in startle magnitude. Delta PPI
25 avoids this eventual flaw by calculating absolute differences between startle magnitudes on pulse-
26 alone and prepulse+pulse trials [73-75]. When we used this parameter, CNO significantly
27 deteriorated PPI performance following FST and RS, irrespective of PCE (FST: 2way ANOVA, Gq-
28 DREADD: $F_{1,66} = 4.23$; $p < 0.05$, Fig. 4E; RS: 2way ANOVA, Gq-DREADD: $F_{1,61} = 47.25$; $p = 0.0001$, Fig.
29
30
31
32
33
34
35
36
37
38
39
40
41
42
43
44
45
46
47
48
49
50
51
52
53
54
55
56
57
58
59
60
61
62
63
64
65

1
2 4F). Therefore, chemogenetic modulation of VTA dopamine neuronal activity is essential for the
3 manifestation of stress-induced impairments of PPI in rats.
4
5
6

7 8 **3.4 Pharmacological correction of stress-induced impairments of gating functions in PCE** 9 **male progeny**

10
11 We previously found that post-natal treatment with neurosteroid pregnenolone (PREG), FDA-
12 approved for clinical trials, prevents PCE-induced hyperdopaminergic phenotypes **only exhibited by**
13 **male progeny** and confers them resilience against acute effects of THC [36]. To test whether PREG
14 precludes stress-induced effects on PPI in PCE male progeny, we administered it (6 mg/kg s.c. once
15 daily for 9 days, from post-natal day -PND- 15 to 23) to CTRL and PCE male rats. Two days following
16 the last administration, when PREG was cleared from the brain, we subjected the animals to FST
17 and PPI (Fig. 5A). In agreement with our previous findings pointing to restorative actions of PREG
18 towards dopamine system function [36], we did not observe **effects on the startle amplitude (2way**
19 **ANOVA PCE x PREG: $F_{1,51} = 1.427$; $p=0.23$; Fig. 5B) while PREG prevented stress-induced**
20 **disruption** of sensorimotor gating functions in PCE male offspring (2way ANOVA PCE x PREG: $F_{1,47}$
21 $= 8.803$; $p=0.0047$, Fig. 5C). PREG treatment had no effect on PPI performance in CTRL male rats
22 (CTRL-VEH vs. CTRL-PREG, $p=0.68$). PREG can also act by inhibiting the GSK3 β [76], which is a
23 key element in the pathogenesis of schizophrenia [77], and also a target of lithium [78, 79]. We,
24 therefore, tested the hypothesis that PREG molecular target was GSK3 β and that a postnatal
25 treatment with lithium could mimic PREG effects on stress-induced **impairment** of PPI in PCE males.
26 Lithium was administered to CTRL and PCE male rats (50 mg/kg s.c., once daily for 9 days, from
27 PND 15 to 23; Fig. 5D), and 48 hours following the last administration, we subjected the animals to
28 FST and PPI. Notably, lithium **treatment had no effect on startle amplitude in PCE male offspring**
29 **(Fig. 5E; 2way ANOVA PCE x Lithium $F_{1,27} = 0.50$; $p=0.48$) and** rescued PCE males from FST-
30 induced **disruption** without affecting CTRL PPI performance (Fig. 5F; 2way ANOVA PCE x Lithium:
31 $F_{1,28} = 5,100$; $p=0.03$).
32
33
34
35
36
37
38
39
40
41
42
43
44
45
46
47
48
49
50
51
52
53
54
55
56
57
58
59
60
61
62
63
64
65

4. Discussion

1
2
3 In the present study, we demonstrate the essential role of dopamine in the detrimental effects of
4 acute unescapable stressors on sensorimotor gating functions in preadolescent rats. DREADD-
5 driven changes of VTA dopamine cell activity before the exposure to an acute inescapable stressor
6
7 impact on subsequent PPI performance. This highlights the causal link between VTA dopamine
8
9 signaling and the engagement of HPA axis for the individual ability to inhibit behavioral responses to
10
11 incoming sensory information. As PCE promotes a male-specific dysregulation of dopamine and HPA
12
13 axis responses within the VTA (present data and [36, 37]), such stress- and dopamine- induced
14
15 impairment of sensorimotor gating functions only manifest in the male progeny. This is relevant
16
17 because PCE children exhibit proneness to psychotic-like experiences and some
18
19 psychopathological phenotypes where males face a higher risk [20, 23, 28, 80-82].
20
21
22
23
24

25
26 Our data support and extend previous findings suggesting that any manipulation leading to enhanced
27
28 presynaptic dopamine release and/or dopamine receptor stimulation in the target region of the
29
30 Nucleus Accumbens (NAc) disrupts PPI [59, 64, 83-87]. Of note, an association exists between
31
32 hyper- and hypo- activation of mesolimbic and mesocortical dopamine pathways, respectively, and
33
34 the inability of filter out relevant environmental stimuli to control adaptive motor behavior [60, 88].
35
36 Since a bidirectional chemogenetic modulation of dopamine neuronal activity in *TH::Cre* rats also
37
38 modifies dopamine release in the NAc [67], it is plausible that CNO by engaging either Gi- or Gq-
39
40 DREADD corrects or produces, respectively, a mesolimbic hyperdopaminergia, a signature of
41
42 disrupted sensorimotor gating functions [38-41]. Our findings are in line with the evidence that
43
44 hyperdopaminergic resting-states of VTA dopamine cells are necessary in the pathophysiology of
45
46 psychosis and schizophrenia [89-92], and that chemogenetic approaches aimed at normalizing
47
48 rather than silencing VTA dopamine neuronal activity prevent the expression of aberrant behaviors
49
50 in animal models of schizophrenia [91, 92]. Accordingly, PCE in rodents produces male-specific
51
52 hyper-dopaminergic neurophysiological phenotypes [36, 37, 93, 94], shifts the proportion of tonically
53
54 firing dopamine cells [44] and the balance between excitation and inhibition [36, 94], which are
55
56 collectively risk factors for susceptibility to diverse neuropsychiatric disorders. Since acute stress
57
58
59
60
61
62
63
64
65

1 activates dopamine system function, which contributes to homeostatic neurobehavioral stress
2 responses also by altering its sensitivity to subsequent stimuli [8, 12-14, 16, 56, 95, 96], PCE-induced
3 sex-specific derangement of dopamine neuron resting-states may be critical for subsequent
4 susceptibility to develop psychopathological phenotypes later in life [28, 97-102]. Of note, PCE
5 produces enduring remarkable repercussions in the offspring that go beyond the brain-wide
6 adaptations, including alterations in lipidomic and cytokine/chemokine profiles [94, 99, 100, 103-
7 105], and extend from cardiac and metabolic dysfunction to changes in intestinal microbiota
8 composition [104, 106]. Since gut microbiota couples immune responses to stress-sensitive brain
9 circuits [107], these findings warrant further investigations to disentangle the mechanisms
10 underpinning PCE sequelae on the progeny and raise concerns on whether these aberrant stress-
11 dependent neurobehavioral reactions (present data and [37, 44]) relate to PCE impact on gut
12 microbiota, lipid and/or glucose metabolism [94, 104], and/or immune system [103], and whether
13 they do subside with development.
14
15
16
17
18
19
20
21
22
23
24
25
26
27
28

29 While the mechanisms underlying PCE sex-specific **changes in the** sensitivity to an acute stressor
30 remain to be fully elucidated, our observations support the notion that an efficient on/off switch
31 mediated by CORT via MR/GR activation is crucial for successful coping and adapting strategies to
32 inescapable stressful situations [7, 108], thereby providing energy for resilience. Indeed, the
33 observation that, in the VTA, PCE male rats only display enhanced and decreased gene expression
34 levels of MRs and GRs, respectively, might explain the sex-specific failure to adopt coping/adaptive
35 strategies during the FST [37, 44]. Accordingly, a less efficient termination of the HPA axis activity
36 mediated by GRs, which operate as the off-switch **[7, 52, 55]**, promotes energy expenditure and
37 exaggerated behavioral responses [7, 52]. Conversely, our finding that acute FST only in PCE
38 females increases gene expression levels of MRs, without affecting those of GRs, supports the
39 notion that a gain-of-function of MRs combined with an efficient GR-dependent off-switch is
40 associated with a “resilient” phenotype better equipped for acute stress responses of the HPA axis
41 and for long-term adaptation [7, 52, 55]. Accordingly, while acute stress increases plasma CORT and
42 ACTH levels to a larger extent in females when compared to males (present data and [54]), and
43 CORT is detrimental to PPI performance [109] (Fig. 1B), acute FST does not affect PPI in PCE
44
45
46
47
48
49
50
51
52
53
54
55
56
57
58
59
60
61
62
63
64
65

1 female rats, which also show appropriate coping strategies during the FST [37]. Consequently, PCE-
2 induced male-specific MR/GR imbalances within the VTA may take part to those metaplastic
3 changes setting a resting state prone to maladaptive stress reaction and PPI deterioration, the latter
4 requiring a hyperdopaminergic neurophysiological phenotype.
5
6
7

8
9 Finally, our study helps elucidating the mechanisms participating in sex-dependent PCE detrimental
10 effects on PPI performance by establishing that these behavioral effects depend on abnormal GPCR
11 signaling cascade engaged in VTA dopamine neurons, including GSK-3 β , a molecular signature of
12 diverse psychiatric conditions [77, 110-113]. Our results showing that PREG, which also inhibits the
13 GSK-3 β [114], corrects FST-induced **disruption** of PPI in PCE male offspring extend previous
14 evidence that it can restore VTA dopamine circuit function and its responsiveness to an acute
15 challenge of THC in PCE males [36]. Since PREG restorative effects are manifest in its absence
16 (present data and [36]), cannot be ascribed to its well-known downstream metabolites (e.g.,
17 progesterone) [36], and are mimicked by lithium, our data **might suggest, among the many others,**
18 GSK-3 β as a possible molecular target candidate. Given that Gi-DREADD stimulation in VTA
19 dopamine cells of PCE male rats rescues the aberrant phenotype, one **is tempted to speculate** the
20 occurrence of a molecular convergence that involves hyperactivity of GSK-3 β as an adaptive
21 response to PCE. This **would be** in line with the role of GSK3 β in neurodevelopment [115], in the
22 pathogenesis of diverse psychiatric disorders (mood disorders, schizophrenia, drug abuse) [112,
23 113, 116-118] and in response to medication [78, 119-121]. Thus, while inhibiting its activity is
24 considered of therapeutic interest, **our study warrants further investigation into the effects of PCE on**
25 **this molecular target.**
26
27
28
29
30
31
32
33
34
35
36
37
38
39
40
41
42
43
44
45
46

47 As cannabis use among pregnant women has been on the rise [30, 31], our study deepens the
48 knowledge on PCE detrimental effects on neurodevelopment [26, 81] and warrants further
49 investigations on the extensive spectrum of neurobehavioral maladaptations induced by the different
50 ingredients of cannabis and at different developmental stages to uncover age- and gender-specific
51 therapeutic approaches.
52
53
54
55
56
57
58
59
60
61
62
63
64
65

5. Conclusions

Given the well-established interplay between stressful life events and the onset of psychopathologies, particularly during (pre)adolescence, our study helps delineating neuroendocrine mechanisms connecting, for the first time to our knowledge, stress and dopamine-dependent psychopathologies.

6. Acknowledgements

The authors thank S. Aramo, and the CeSASst personnel for their skillful assistance.

7. Author contributions

V.S., F.T., and L.C. performed behavioral experiments and analyzed the data. V.S., S.A., and R.L. performed the surgeries. P.P. and L.P-V. carried out the molecular experiments and analyzed the data. A.B-G., P.P. and R.F. analyzed molecular and behavioral data, and reviewed the manuscript. M.S. and R.L. carried out immunohistochemical experiments and analyzed the data. V.S. and R.L. prepared the figures. M.M. conceived, designed and supervised the project, provided funding and wrote the original draft.

8. Funding sources

The present study was funded by the Horizon Europe 2022 Excellent Science - European Research Council (101088207 to M.M.). A.B-G. and L.P-V. received funding from the DIUE de la Generalitat de Catalunya (SGR 00022, 2023 FI-3 00034) and from the H2020 Excellent Science - European Research Council (948217 to A.B-G.).

9. Figure legends

Figure 1. Sex-specific effects of acute stress on sensorimotor gating function. A) Timeline of experimental procedures for pre-pulse inhibition (PPI) experiments (top) and blood collection

(bottom). **B)** Forced swim test (FST) differentially impacts on sensorimotor gating functions in male and female rats (*p = 0.036 CTRL males vs. PCE males-**shaded grey area**; **p = 0.003 CTRL males vs. CTRL females; Sidak's test; n_{rats} = 7 CTRL **females**, 9 PCE females, 15 CTRL **males**, 16 PCE males). **C)** Corticosterone and **D)** adrenocorticotrophic hormone (ACTH) concentrations were measured from plasma samples collected from unstressed rats and from stressed rats after 30 min from the beginning of the FST: *CORT*: *p = 0.01 stressed CTRL males vs. stressed CTRL females; **p = 0.003 stressed PCE males vs. stressed PCE females. *ACTH*: **p = 0.006 stressed CTRL males vs. stressed CTRL females; Sidak's test. Data are expressed as ng/ml of plasma and obtained from **7 unstressed and 8 stressed CTRL males, 6 unstressed and 7 stressed CTRL females, 12 unstressed and stressed PCE males, 7 unstressed and 9 stressed PCE females**. Unless otherwise indicated, data are represented with scatter plots with mean and ± SEM. Figure created with BioRender.com.

Figure 2. Feedback sensitivity to acute stress is reduced in PCE males. **A)** Timeline of experimental procedures. **The quantitative real-time PCR analysis of gene expression levels of MR (Nr3c2) and GR (Nr3c1) were measured from VTA tissue punches collected from unstressed rats and from stressed rats after 30 min from the beginning of the forced swim test (FST).** **B)** Fold change ratio of mRNA expression levels of Nr3c2 in VTA of males at preadolescence from unstressed rats and from stressed rats after the FST (*p = 0.0113 main effect of PCE; n_{rats} = 9 **naïve (unstressed) and 6 stressed** CTRL males, 13 **unstressed and 9 stressed** PCE males). **C)** Graphs show the mRNA expression levels of Nr3c1 in VTA as a fold change ratio in **PCE** male rats compared with their corresponding control group, **in both** unstressed or stressed rats (**p = 0.0054 main effect of PCE; *p = 0,04 main effect of stress- **shaded grey area**; n_{rats} = 10 **unstressed and 7 stressed** CTRL males, 17 **unstressed and 14 stressed** PCE males). **D)** Fold change ratio of mRNA expression levels of Nr3c2 in VTA of unstressed and stressed females at preadolescence (* p < 0.05 stressed PCE vs. stressed CTRL- **shaded grey area**; Sidak's test; n_{rats} = 9 **unstressed and 6 stressed** CTRL females, 10 **unstressed and 4 stressed** PCE females). **E)** Graphs show the mRNA expression levels of Nr3c1 in VTA as a fold change ratio in stressed and unstressed **PCE** female rats compared with their corresponding control group (n_{rats} = 9 **unstressed and 6 stressed** CTRL females, 10 **unstressed and**

8 stressed PCE females). Unless otherwise indicated, data are represented with scatter plots with
1
2 mean and \pm SEM. Figure created with BioRender.com.

3
4
5 **Figure 3. Maladaptive responses to acute stress are mediated by VTA dopaminergic activity.**

6
7 **A)** Schematic timeline of PCE treatment and behavioral experiments. *TH::Cre* positive male offspring
8 rats were bilaterally injected with AAV5-hSyn-DIO-hM4D(Gi)-mCherry or control virus (AAV5-hSyn-
9 DIO-mCherry) in the VTA at PND7. After 3 weeks, male offspring were injected with clozapine N-
10 Oxide (CNO), then after an acute stress rats were exposed to pre pulse inhibition test (PPI). CNO
11 administration occurred 30 min before the PPI. **B)** Representative fluorescent images of Gi-mCherry
12 and TH positive cells in coronal brain sections containing the VTA, counterstained for DAPI (left
13 panel). Yellow square indicates one example of ROI used for cell count (left panel). Scale bar, 250
14 μ M. High magnification of yellow ROI for labelling quantification in VTA (top right): arrows indicate
15 cells double positive for TH (green) and Gi-mCherry (red). Scale bar, 25 μ M. Pie charts showing the
16 proportions of Gi-mCherry positive (red) and TH/Gi-mCherry positive cells (yellow) within sampled
17 ROIs in CTRL and PCE animals (bottom right). **C)** Forced swim test (FST) does not affect the startle
18 amplitude. Startle amplitude values are represented as arbitrary units (AU). (n_{rats} = 7 PCE-control;
19 10 PCE-Gi; 11 CTRL- control; 13 CTRL-Gi). **D)** Gi-DREADD activation prevents FST-induced
20 impairment of sensorimotor gating functions in PCE males (** $p=0.001$ CTRL-control vs PCE-control-
21 shaded grey area; Sidak's test; n_{rats} = 10 PCE-Gi; 16 CTRL-control and PCE-control; 21 CTRL-Gi).
22 **E)** Effect of acute restraint stress (RS) in the startle amplitude after Gi-DREADD activation in PCE
23 male offspring (n_{rats} = 10 CTRL- control and PCE- Gi; 13 CTRL-Gi; 7 PCE-control). **F)** Gi-DREADD
24 activation prevents PPI impairment exhibited by PCE males (* $p=0.04$ CTRL-control vs PCE-control-
25 shaded grey area; Sidak's test; n_{rats} = 9 PCE-Gi; 10 CTRL- control and PCE-control; 12 CTRL-Gi).
26 Unless otherwise indicated, data are represented with scatter plots with mean and \pm SEM. Figure
27 created with BioRender.com.

28
29
30
31
32
33
34
35
36
37
38
39
40
41
42
43
44
45
46
47
48
49
50
51
52
53
54
55
56 **Figure 4. Chemogenetic activation of VTA DA neurons induces maladaptive responses to**

57 acute stress in female rats. **A)** Schematic timeline of PCE treatment and behavioral experiments.
58 *TH::Cre* positive female offspring rats were bilaterally injected with AAV5-hSyn-DIO-hM3D(Gq)-
59

1 mCherry or control virus (AAV5-hSyn-DIO-mCherry) in the VTA at PND7. After 3 weeks, female
2 offspring were injected with clozapine N-Oxide (CNO), then after an acute stress rats were exposed
3 to pre pulse inhibition test (PPI). CNO administration occurred 30 min before the PPI. **B)**
4 Representative fluorescent images of Gq-mCherry and TH positive cells in coronal brain sections
5 containing the VTA, counterstained for DAPI (left panel). Yellow square indicates one example ROI
6 used for cell count (left panel). Scale bar, 250 μ M. High magnification of yellow ROI for labelling
7 quantification in VTA (top right): arrows indicate cells double positive for TH (green) and Gq-mCherry
8 (red). Pie charts showing the proportions of Gq-mCherry positive (red) and TH/Gq-mCherry positive
9 cells (yellow) within sampled ROIs in CTRL and PCE animals (bottom right). Scale bar, 25 μ M. **C)**
10 Gq-DREADD activation affects the startle amplitude in control female offspring after FST. Startle
11 amplitude values are represented as arbitrary units (AU) (* $p=0,019$ main effect of Gq; $n_{rats} = 16$
12 CTRL- control; 21 PCE-control; 17 CTRL-Gq; 16 PCE-Gq). **D)** Effect of Gq-DREADD activation in
13 the startle amplitude after the exposure to an acute restraint stress (RS) in female rats (**** $p < 0.0001$
14 main effect of Gq; $n_{rats} = 16$ CTRL- control, PCE-control and PCE-Gq; 17 CTRL-Gq). **E)** Gq-DREADD
15 activation impairs sensorimotor gating functions following FST in female rats (* $p=0,04$ main effect of
16 Gq; $n_{rats} = 16$ CTRL- control and PCE-Gq; 21 PCE-control; CTRL-Gq). **F)** Gq-DREADD activation
17 induces PPI impairment in response to RS in female rats (**** $p < 0.0001$ main effect of Gq; $n_{rats} =$
18 16 CTRL- control and PCE-control; 17 CTRL-Gq; 16 PCE-Gq). Unless otherwise indicated, data are
19 represented with scatter plots with mean and \pm SEM. Figure created with BioRender.com.

20 **Figure 5. Pharmacological manipulations with pregnenolone or lithium prevent stress-**
21 **induced impairment of gating functions in PCE male progeny. A)** Schematic timeline of PCE
22 treatment and subchronic treatment with pregnenolone (PREG). **B)** Effect of PREG on the startle
23 amplitude after forced swim test (FST) in PCE male offspring. Startle amplitude values are
24 represented as arbitrary units (AU) ($n_{rats} = 10-13$ CTRL/PCE-PREG; 16 CTRL/PCE-VEH). **C)** PREG
25 prevents forced swim test (FST)-induced impairment of pre-pulse inhibition (PPI) in male PCE
26 offspring (* $p=0.02$ PCE-VEH vs. CTRL-VEH; * $p=0.01$ PCE-VEH vs. PCE-PREG; Tukey's test; n_{rats}
27 = 9 CTRL/PCE-PREG; 16-17 CTRL/PCE-VEH). **D)** Schematic timeline of PCE treatment and

subchronic treatment with lithium. **E) Effect of lithium on the startle amplitude after forced swim test (FST) in PCE male offspring.** Startle amplitude values are represented as arbitrary units (AU) ($n_{rats} = 7-8$ CTRL/PCE-Lithium; $8-9$ CTRL/PCE-VEH). **F) Lithium prevents FST-induced impairment of PPI in male PCE offspring** (** $p=0.003$ PCE-VEH vs. CTRL-VEH; Tukey's test; $n_{rats} = 7-8$ CTRL/PCE-Lithium; $8-9$ CTRL/PCE-VEH). Unless otherwise indicated, data are represented with scatter plots with mean and \pm SEM. Figure created with BioRender.com.

10. References

- [1] GBD 2017 Disease and Injury Incidence and Prevalence Collaborators. Global, regional, and national incidence, prevalence, and years lived with disability for 354 diseases and injuries for 195 countries and territories, 1990–2017: a systematic analysis for the Global Burden of Disease Study 2017. , *The Lancet* (2018).
- [2] M. Solmi, J. Radua, M. Olivola, E. Croce, L. Soardo, G. Salazar de Pablo, J. Il Shin, J.B. Kirkbride, P. Jones, J.H. Kim, J.Y. Kim, A.F. Carvalho, M.V. Seeman, C.U. Correll, P. Fusar-Poli, Age at onset of mental disorders worldwide: large-scale meta-analysis of 192 epidemiological studies, *Mol Psychiatry* 27(1) (2022) 281-295.
- [3] A. Caspi, R.M. Houts, A. Ambler, A. Danese, M.L. Elliott, A. Hariri, H. Harrington, S. Hogan, R. Poulton, S. Ramrakha, L.J.H. Rasmussen, A. Reuben, L. Richmond-Rakerd, K. Sugden, J. Wertz, B.S. Williams, T.E. Moffitt, Longitudinal Assessment of Mental Health Disorders and Comorbidities Across 4 Decades Among Participants in the Dunedin Birth Cohort Study, *JAMA Netw Open* 3(4) (2020) e203221.
- [4] W.H. Organization, *The World Health Report: 2001: Mental Health: New Understanding, New Hope.* World Health Organization., (2001).
- [5] I. Pereira-Figueiredo, E. Umeoka, Stress: Influences and Determinants of Psychopathology., *Encyclopedia* 4(2) (2024) 1026-1043.
- [6] E. Nederhof, F.V. van Oort, E.M. Bouma, O.M. Laceulle, A.J. Oldehinkel, J. Ormel, Predicting mental disorders from hypothalamic-pituitary-adrenal axis functioning: a 3-year follow-up in the TRAILS study, *Psychol Med* 45(11) (2015) 2403-12.
- [7] E.R. de Kloet, M. Joels, The cortisol switch between vulnerability and resilience, *Mol Psychiatry* 29(1) (2024) 20-34.
- [8] M.A. Bloomfield, R.A. McCutcheon, M. Kempton, T.P. Freeman, O. Howes, The effects of psychosocial stress on dopaminergic function and the acute stress response, *Elife* 8 (2019).
- [9] J.H. Baik, Stress and the dopaminergic reward system, *Exp Mol Med* 52(12) (2020) 1879-1890.
- [10] H.C. Meyer, F.S. Lee, Translating Developmental Neuroscience to Understand Risk for Psychiatric Disorders, *Am J Psychiatry* 176(3) (2019) 179-185.
- [11] M. Mandy, M. Nyirenda, Developmental Origins of Health and Disease: the relevance to developing nations, *Int Health* 10(2) (2018) 66-70.
- [12] E.H. Douma, E.R. de Kloet, Stress-induced plasticity and functioning of ventral tegmental dopamine neurons, *Neurosci Biobehav Rev* 108 (2020) 48-77.
- [13] E.N. Holly, K.A. Miczek, Ventral tegmental area dopamine revisited: effects of acute and repeated stress, *Psychopharmacology (Berl)* 233(2) (2016) 163-86.
- [14] O. Valenti, D.J. Lodge, A.A. Grace, Aversive stimuli alter ventral tegmental area dopamine neuron activity via a common action in the ventral hippocampus, *J Neurosci* 31(11) (2011) 4280-9.
- [15] J.L. Niehaus, M. Murali, J.A. Kauer, Drugs of abuse and stress impair LTP at inhibitory synapses in the ventral tegmental area, *Eur J Neurosci* 32(1) (2010) 108-17.

- 1 [16] D. Saal, Y. Dong, A. Bonci, R.C. Malenka, Drugs of abuse and stress trigger a common
2 synaptic adaptation in dopamine neurons, *Neuron* 37(4) (2003) 577-82.
- 3 [17] J.C. Pruessner, F. Champagne, M.J. Meaney, A. Dagher, Dopamine release in response to a
4 psychological stress in humans and its relationship to early life maternal care: a positron emission
5 tomography study using [¹¹C]raclopride, *J Neurosci* 24(11) (2004) 2825-31.
- 6 [18] M. Colizzi, A. Lasalvia, M. Ruggeri, Prevention and early intervention in youth mental health: is
7 it time for a multidisciplinary and trans-diagnostic model for care?, *Int J Ment Health Syst* 14 (2020)
8 23.
- 9 [19] K. Bolhuis, M.E. Koopman-Verhoeff, L.M.E. Blanken, D. Cibrev, V.W.V. Jaddoe, F.C. Verhulst,
10 M.H.J. Hillegers, S.A. Kushner, H. Tiemeier, Psychotic-like experiences in pre-adolescence: what
11 precedes the antecedent symptoms of severe mental illness?, *Acta Psychiatr Scand* 138(1) (2018)
12 15-25.
- 13 [20] J.D. Fine, A.L. Moreau, N.R. Karcher, A. Agrawal, C.E. Rogers, D.M. Barch, R. Bogdan,
14 Association of Prenatal Cannabis Exposure With Psychosis Proneness Among Children in the
15 Adolescent Brain Cognitive Development (ABCD) Study, *JAMA Psychiatry* (2019).
- 16 [21] S.E. Paul, A.S. Hatoum, J.D. Fine, E.C. Johnson, I. Hansen, N.R. Karcher, A.L. Moreau, E.
17 Bondy, Y. Qu, E.B. Carter, C.E. Rogers, A. Agrawal, D.M. Barch, R. Bogdan, Associations Between
18 Prenatal Cannabis Exposure and Childhood Outcomes: Results From the ABCD Study, *JAMA*
19 *Psychiatry* (2020).
- 20 [22] S. Singh, K.B. Filion, H.A. Abenham, M.J. Eisenberg, Prevalence and outcomes of prenatal
21 recreational cannabis use in high-income countries: a scoping review, *BJOG* 127(1) (2020) 8-16.
- 22 [23] A.W. Tadesse, G. Ayano, B.A. Dachew, K. Betts, R. Alati, Exposure to maternal cannabis use
23 disorder and risk of autism spectrum disorder in offspring: A data linkage cohort study, *Psychiatry*
24 *Res* 337 (2024) 115971.
- 25 [24] M.M. Faraj, J. Evanski, C.G. Zundel, C. Peters, S. Brummelte, L. Lundahl, H.A. Marusak,
26 Impact of prenatal cannabis exposure on functional connectivity of the salience network in children,
27 *J Neurosci Res* 101(1) (2023) 162-171.
- 28 [25] N.D. Volkow, W.M. Compton, E.M. Wargo, The Risks of Marijuana Use During Pregnancy,
29 *Jama* 317(2) (2017) 129-130.
- 30 [26] A.W. Tadesse, B.A. Dachew, G. Ayano, K. Betts, R. Alati, Prenatal cannabis use and the risk of
31 attention deficit hyperactivity disorder and autism spectrum disorder in offspring: A systematic
32 review and meta-analysis, *J Psychiatr Res* 171 (2024) 142-151.
- 33 [27] R.D. Eiden, S. Shisler, D.A. Granger, P. Schuetze, J. Colangelo, M.A. Huestis, Prenatal
34 Tobacco and Cannabis Exposure: Associations with Cortisol Reactivity in Early School Age
35 Children, *Int J Behav Med* 27(3) (2020) 343-356.
- 36 [28] G. Rompala, Y. Nomura, Y.L. Hurd, Maternal cannabis use is associated with suppression of
37 immune gene networks in placenta and increased anxiety phenotypes in offspring, *Proc Natl Acad*
38 *Sci U S A* 118(47) (2021).
- 39 [29] L.R. Stroud, G.D. Papandonatos, N.C. Jao, C. Vergara-Lopez, M.A. Huestis, A.L. Salisbury,
40 Prenatal tobacco and marijuana co-use: Sex-specific influences on infant cortisol stress response,
41 *Neurotoxicol Teratol* 79 (2020) 106882.
- 42 [30] S. Hayes, E. Delker, G. Bandoli, The prevalence of cannabis use reported among pregnant
43 individuals in the United States is increasing, 2002-2020, *J Perinatol* 43(3) (2023) 387-389.
- 44 [31] Q.L. Brown, A.L. Sarvet, D. Shmulewitz, S.S. Martins, M.M. Wall, D.S. Hasin, Trends in
45 Marijuana Use Among Pregnant and Nonpregnant Reproductive-Aged Women, 2002-2014, *Jama*
46 317(2) (2017) 207-209.
- 47 [32] N.D. Volkow, B. Han, W.M. Compton, E.F. McCance-Katz, Self-reported Medical and
48 Nonmedical Cannabis Use Among Pregnant Women in the United States, *Jama* 322(2) (2019)
49 167-169.
- 50 [33] B. Dickson, C. Mansfield, M. Guiahi, A.A. Allshouse, L.M. Borgelt, J. Sheeder, R.M. Silver, T.D.
51 Metz, Recommendations From Cannabis Dispensaries About First-Trimester Cannabis Use,
52 *Obstet Gynecol* 131(6) (2018) 1031-1038.
- 53 [34] M. O'Connor, Medicinal Cannabis in Pregnancy - Panacea or Noxious Weed?, *J Law Med*
54 25(3) (2018) 634-646.
- 55 [35] M. Besse, K. Parikh, K. Mark, Reported Reasons for Cannabis Use Before and After
56 Pregnancy Recognition, *J Addict Med* 17(5) (2023) 563-567.

- 1 [36] R. Frau, V. Miczán, F. Traccis, S. Aroni, C.I. Pongor, P. Saba, V. Serra, C. Sagheddu, S. Fanni,
2 M. Congiu, P. Devoto, J.F. Cheer, I. Katona, M. Melis, Prenatal THC produces a
3 hyperdopaminergic phenotype rescued by pregnenolone, *Nat Neurosci* 22(12) (2019) 11.
- 4 [37] F. Traccis, V. Serra, C. Sagheddu, M. Congiu, P. Saba, G. Giua, P. Devoto, R. Frau, J.F.
5 Cheer, M. Melis, Prenatal THC Does Not Affect Female Mesolimbic Dopaminergic System in
6 Preadolescent Rats, *Int J Mol Sci* 22(4) (2021).
- 7 [38] J.G. Howland, E.M. MacKenzie, T.T. Yim, P. Taepavarapruk, A.G. Phillips, Electrical stimulation
8 of the hippocampus disrupts prepulse inhibition in rats: frequency- and site-dependent effects,
9 *Behav Brain Res* 152(2) (2004) 187-97.
- 10 [39] J.E. Lisman, J.T. Coyle, R.W. Green, D.C. Javitt, F.M. Benes, S. Heckers, A.A. Grace, Circuit-
11 based framework for understanding neurotransmitter and risk gene interactions in schizophrenia,
12 *Trends Neurosci* 31(5) (2008) 234-42.
- 13 [40] D.J. Lodge, A.A. Grace, Aberrant hippocampal activity underlies the dopamine dysregulation in
14 an animal model of schizophrenia, *The Journal of neuroscience : the official journal of the Society*
15 *for Neuroscience* 27(42) (2007) 11424-30.
- 16 [41] N.R. Swerdlow, G.A. Light, Sensorimotor gating deficits in schizophrenia: Advancing our
17 understanding of the phenotype, its neural circuitry and genetic substrates, *Schizophr Res* 198
18 (2018) 1-5.
- 19 [42] J.P. Vargas, E. Diaz, M. Portavella, J.C. Lopez, Animal Models of Maladaptive Traits:
20 Disorders in Sensorimotor Gating and Attentional Quantifiable Responses as Possible
21 Endophenotypes, *Front Psychol* 7 (2016) 206.
- 22 [43] M.A. Geyer, K. Krebs-Thomson, D.L. Braff, N.R. Swerdlow, Pharmacological studies of
23 prepulse inhibition models of sensorimotor gating deficits in schizophrenia: a decade in review,
24 *Psychopharmacology (Berl)* 156(2-3) (2001) 117-54.
- 25 [44] C. Sagheddu, F. Traccis, V. Serra, M. Congiu, R. Frau, J.F. Cheer, M. Melis, Mesolimbic
26 dopamine dysregulation as a signature of information processing deficits imposed by prenatal THC
27 exposure, *Prog Neuropsychopharmacol Biol Psychiatry* 105 (2021) 110128.
- 28 [45] J.L. Wiley, M. O'Connell M, M.E. Tokarz, M.J. Wright, Jr., Pharmacological effects of acute and
29 repeated administration of Delta(9)-tetrahydrocannabinol in adolescent and adult rats, *J Pharmacol*
30 *Exp Ther* 320(3) (2007) 1097-105.
- 31 [46] Z. Mehmedic, S. Chandra, D. Slade, H. Denham, S. Foster, A.S. Patel, S.A. Ross, I.A. Khan,
32 M.A. ElSohly, Potency trends of Delta9-THC and other cannabinoids in confiscated cannabis
33 preparations from 1993 to 2008, *J Forensic Sci* 55(5) (2010) 1209-17.
- 34 [47] C. Klein, E. Karanges, A. Spiro, A. Wong, J. Spencer, T. Huynh, N. Gunasekaran, T. Karl, L.E.
35 Long, X.F. Huang, K. Liu, J.C. Arnold, I.S. McGregor, Cannabidiol potentiates Delta(9)-
36 tetrahydrocannabinol (THC) behavioural effects and alters THC pharmacokinetics during acute and
37 chronic treatment in adolescent rats, *Psychopharmacology (Berl)* 218(2) (2011) 443-57.
- 38 [48] D.M. Schwoppe, E.L. Karschner, D.A. Gorelick, M.A. Huestis, Identification of recent cannabis
39 use: whole-blood and plasma free and glucuronidated cannabinoid pharmacokinetics following
40 controlled smoked cannabis administration, *Clin Chem* 57(10) (2011) 1406-14.
- 41 [49] M. Falcon, S. Pichini, J. Joya, M. Pujadas, A. Sanchez, O. Vall, O. Garcia Algar, A. Luna, R. de
42 la Torre, M.C. Rotolo, M. Pellegrini, Maternal hair testing for the assessment of fetal exposure to
43 drug of abuse during early pregnancy: Comparison with testing in placental and fetal remains,
44 *Forensic Sci Int* 218(1-3) (2012) 92-6.
- 45 [50] W.C. Paxinos G, *The rat brain in stereotaxic coordinates*, 6th Edition ed., Academic Press,
46 San Diego, CA, 2007.
- 47 [51] G. Boero, M.G. Pisu, F. Biggio, L. Muredda, G. Carta, S. Banni, E. Paci, P. Follesa, A. Concas,
48 P. Porcu, M. Serra, Impaired glucocorticoid-mediated HPA axis negative feedback induced by
49 juvenile social isolation in male rats, *Neuropharmacology* 133 (2018) 242-253.
- 50 [52] A.P. Harris, M.C. Holmes, E.R. de Kloet, K.E. Chapman, J.R. Seckl, Mineralocorticoid and
51 glucocorticoid receptor balance in control of HPA axis and behaviour, *Psychoneuroendocrinology*
52 38(5) (2013) 648-58.
- 53 [53] K.A. Richardson, A.K. Hester, G.L. McLemore, Prenatal cannabis exposure - The "first hit" to
54 the endocannabinoid system, *Neurotoxicol Teratol* 58 (2016) 5-14.
- 55 [54] M.B. Solomon, M. Loftspring, A.D. de Kloet, S. Ghosal, R. Jankord, J.N. Flak, A.C. Wulsin,
56 E.G. Krause, R. Zhang, T. Rice, J. McKlveen, B. Myers, J.G. Tasker, J.P. Herman, *Neuroendocrine*
57
58
59
60
61
62
63
64
65

Function After Hypothalamic Depletion of Glucocorticoid Receptors in Male and Female Mice, *Endocrinology* 156(8) (2015) 2843-53.

[55] E.R. de Kloet, Brain mineralocorticoid and glucocorticoid receptor balance in neuroendocrine regulation and stress-related psychiatric etiopathologies, *Curr Opin Endocr Metab Res* 24 (2022) 100352.

[56] S.S. Daftary, J. Panksepp, Y. Dong, D.B. Saal, Stress-induced, glucocorticoid-dependent strengthening of glutamatergic synaptic transmission in midbrain dopamine neurons, *Neurosci Lett* 452(3) (2009) 273-6.

[57] A.R. de Oliveira, A.E. Reimer, M.L. Brandao, Mineralocorticoid receptors in the ventral tegmental area regulate dopamine efflux in the basolateral amygdala during the expression of conditioned fear, *Psychoneuroendocrinology* 43 (2014) 114-25.

[58] S.B. Powell, X. Zhou, M.A. Geyer, Prepulse inhibition and genetic mouse models of schizophrenia, *Behav Brain Res* 204(2) (2009) 282-94.

[59] R.S. Mansbach, M.A. Geyer, D.L. Braff, Dopaminergic stimulation disrupts sensorimotor gating in the rat, *Psychopharmacology (Berl)* 94(4) (1988) 507-14.

[60] D.L. Braff, M.A. Geyer, Sensorimotor gating and schizophrenia. Human and animal model studies, *Arch Gen Psychiatry* 47(2) (1990) 181-8.

[61] J.M. Doherty, V.L. Masten, S.B. Powell, R.J. Ralph, D. Klamer, M.J. Low, M.A. Geyer, Contributions of dopamine D1, D2, and D3 receptor subtypes to the disruptive effects of cocaine on prepulse inhibition in mice, *Neuropsychopharmacology* 33(11) (2008) 2648-56.

[62] J. Zhang, C. Forkstam, J.A. Engel, L. Svensson, Role of dopamine in prepulse inhibition of acoustic startle, *Psychopharmacology (Berl)* 149(2) (2000) 181-8.

[63] C. Nasello, L.A. Poppi, J. Wu, T.F. Kowalski, J.K. Thackray, R. Wang, A. Persaud, M. Mahboob, S. Lin, R. Spaseska, C.K. Johnson, D. Gordon, F. Tissir, G.A. Heiman, J.A. Tischfield, M. Bocarsly, M.A. Tischfield, Human mutations in high-confidence Tourette disorder genes affect sensorimotor behavior, reward learning, and striatal dopamine in mice, *Proc Natl Acad Sci U S A* 121(19) (2024) e2307156121.

[64] C. Yang, X. Chen, J. Xu, W. Chen, SKF82958, a dopamine D1 receptor agonist, disrupts prepulse inhibition in the medial prefrontal cortex and nucleus accumbens in C57BL/6J mice, *Behav Pharmacol* 35(4) (2024) 193-200.

[65] B. Acevedo, E. Aron, S. Pospos, D. Jessen, The functional highly sensitive brain: a review of the brain circuits underlying sensory processing sensitivity and seemingly related disorders, *Philos Trans R Soc Lond B Biol Sci* 373(1744) (2018).

[66] A.J. Brown, D.A. Fisher, E. Kouranova, A. McCoy, K. Forbes, Y. Wu, R. Henry, D. Ji, A. Chambers, J. Warren, W. Shu, E.J. Weinstein, X. Cui, Whole-rat conditional gene knockout via genome editing, *Nat Methods* 10(7) (2013) 638-40.

[67] S.V. Mahler, Z.D. Brodnik, B.M. Cox, W.C. Buchta, B.S. Bentzley, J. Quintanilla, Z.A. Cope, E.C. Lin, M.D. Riedy, M.D. Scofield, J. Messinger, C.M. Ruiz, A.C. Riegel, R.A. Espana, G. Aston-Jones, Chemogenetic Manipulations of Ventral Tegmental Area Dopamine Neurons Reveal Multifaceted Roles in Cocaine Abuse, *J Neurosci* 39(3) (2019) 503-518.

[68] S.V. Mahler, E.M. Vazey, J.T. Beckley, C.R. Keistler, E.M. McGlinchey, J. Kaufling, S.P. Wilson, K. Deisseroth, J.J. Woodward, G. Aston-Jones, Designer receptors show role for ventral pallidum input to ventral tegmental area in cocaine seeking, *Nat Neurosci* 17(4) (2014) 577-85.

[69] J.L. Gomez, J. Bonaventura, W. Lesniak, W.B. Mathews, P. Sysa-Shah, L.A. Rodriguez, R.J. Ellis, C.T. Richie, B.K. Harvey, R.F. Dannals, M.G. Pomper, A. Bonci, M. Michaelides, Chemogenetics revealed: DREADD occupancy and activation via converted clozapine, *Science* 357(6350) (2017) 503-507.

[70] L. Boekhoudt, E.C. Wijbrans, J.H.K. Man, M.C.M. Luijendijk, J.W. de Jong, G. van der Plasse, L. Vanderschuren, R.A.H. Adan, Enhancing excitability of dopamine neurons promotes motivational behaviour through increased action initiation, *Eur Neuropsychopharmacol* 28(1) (2018) 171-184.

[71] H.L. Robinson, K.L. Nicholson, K.L. Shelton, P.J. Hamilton, M.L. Banks, Comparison of three DREADD agonists acting on Gq-DREADDs in the ventral tegmental area to alter locomotor activity in tyrosine hydroxylase:Cre male and female rats, *Behav Brain Res* 455 (2023) 114674.

[72] L. Boekhoudt, A. Omrani, M.C. Luijendijk, I.G. Wolterink-Donselaar, E.C. Wijbrans, G. van der Plasse, R.A. Adan, Chemogenetic activation of dopamine neurons in the ventral tegmental area,

1 but not substantia nigra, induces hyperactivity in rats, *Eur Neuropsychopharmacol* 26(11) (2016)
2 1784-1793.
3 [73] M. Bortolato, R. Frau, G.N. Aru, M. Orru, G.L. Gessa, Baclofen reverses the reduction in
4 prepulse inhibition of the acoustic startle response induced by dizocilpine, but not by apomorphine,
5 *Psychopharmacology (Berl)* 171(3) (2004) 322-30.
6 [74] M. Bortolato, R. Frau, M. Orru, M. Collu, G. Mereu, M. Carta, F. Fadda, R. Stancampiano,
7 Effects of tryptophan deficiency on prepulse inhibition of the acoustic startle in rats,
8 *Psychopharmacology (Berl)* 198(2) (2008) 191-200.
9 [75] R. Frau, L.J. Mosher, V. Bini, G. Pillolla, R. Pes, P. Saba, S. Fanni, P. Devoto, M. Bortolato,
10 The neurosteroidogenic enzyme 5alpha-reductase modulates the role of D1 dopamine receptors in
11 rat sensorimotor gating, *Psychoneuroendocrinology* 63 (2016) 59-67.
12 [76] P. Wong, Y. Sze, C.C. Chang, J. Lee, X. Zhang, Pregnenolone sulfate normalizes
13 schizophrenia-like behaviors in dopamine transporter knockout mice through the AKT/GSK3beta
14 pathway, *Transl Psychiatry* 5 (2015) e528.
15 [77] S. Lovestone, R. Killick, M. Di Forti, R. Murray, Schizophrenia as a GSK-3 dysregulation
16 disorder, *Trends Neurosci* 30(4) (2007) 142-9.
17 [78] J.M. Beaulieu, T.D. Sotnikova, W.D. Yao, L. Kockeritz, J.R. Woodgett, R.R. Gainetdinov, M.G.
18 Caron, Lithium antagonizes dopamine-dependent behaviors mediated by an AKT/glycogen
19 synthase kinase 3 signaling cascade, *Proc Natl Acad Sci U S A* 101(14) (2004) 5099-104.
20 [79] P.S. Klein, D.A. Melton, A molecular mechanism for the effect of lithium on development, *Proc*
21 *Natl Acad Sci U S A* 93(16) (1996) 8455-9.
22 [80] K. Bolhuis, S.A. Kushner, S. Yalniz, M.H.J. Hillegers, V.W.V. Jaddoe, H. Tiemeier, H. El
23 Marroun, Maternal and paternal cannabis use during pregnancy and the risk of psychotic-like
24 experiences in the offspring, *Schizophr Res* 202 (2018) 322-327.
25 [81] D.J. Corsi, J. Donelle, E. Sucha, S. Hawken, H. Hsu, D. El-Chaar, L. Bisnaire, D. Fell, S.W.
26 Wen, M. Walker, Maternal cannabis use in pregnancy and child neurodevelopmental outcomes,
27 *Nat Med* 26(10) (2020) 1536-1540.
28 [82] S.E. Paul, A.S. Hatoum, J.D. Fine, E.C. Johnson, I. Hansen, N.R. Karcher, A.L. Moreau, E.
29 Bondy, Y. Qu, E.B. Carter, C.E. Rogers, A. Agrawal, D.M. Barch, R. Bogdan, Associations Between
30 Prenatal Cannabis Exposure and Childhood Outcomes: Results From the ABCD Study, *JAMA*
31 *Psychiatry* 78(1) (2021) 64-76.
32 [83] D.C. Hoffman, H. Donovan, D1 and D2 dopamine receptor antagonists reverse prepulse
33 inhibition deficits in an animal model of schizophrenia, *Psychopharmacology (Berl)* 115(4) (1994)
34 447-53.
35 [84] A.M. McCoy, T.D. Prevot, M.Y. Mian, J.M. Cook, A. Frazer, E.L. Sibille, F.R. Carreno, D.J.
36 Lodge, Positive Allosteric Modulation of alpha5-GABAA Receptors Reverses Stress-Induced
37 Alterations in Dopamine System Function and Prepulse Inhibition of Startle, *Int J*
38 *Neuropsychopharmacol* 25(8) (2022) 688-698.
39 [85] N.R. Swerdlow, R.S. Mansbach, M.A. Geyer, L. Pulvirenti, G.F. Koob, D.L. Braff, Amphetamine
40 disruption of prepulse inhibition of acoustic startle is reversed by depletion of mesolimbic
41 dopamine, *Psychopharmacology (Berl)* 100(3) (1990) 413-6.
42 [86] B.B. Tournier, N. Ginovart, Repeated but not acute treatment with $\Delta(9)$ -tetrahydrocannabinol
43 disrupts prepulse inhibition of the acoustic startle: reversal by the dopamine D(2)/(3) receptor
44 antagonist haloperidol, *Eur Neuropsychopharmacol* 24(8) (2014) 1415-23.
45 [87] S.B. Caine, M.A. Geyer, N.R. Swerdlow, Effects of D3/D2 dopamine receptor agonists and
46 antagonists on prepulse inhibition of acoustic startle in the rat, *Neuropsychopharmacology* 12(2)
47 (1995) 139-45.
48 [88] N.R. Swerdlow, B.K. Lipska, D.R. Weinberger, D.L. Braff, G.E. Jaskiw, M.A. Geyer, Increased
49 sensitivity to the sensorimotor gating-disruptive effects of apomorphine after lesions of medial
50 prefrontal cortex or ventral hippocampus in adult rats, *Psychopharmacology (Berl)* 122(1) (1995)
51 27-34.
52 [89] S. Kapur, Psychosis as a state of aberrant salience: a framework linking biology,
53 phenomenology, and pharmacology in schizophrenia, *Am J Psychiatry* 160(1) (2003) 13-23.
54 [90] O.D. Howes, R. McCutcheon, M.J. Owen, R.M. Murray, The Role of Genes, Stress, and
55 Dopamine in the Development of Schizophrenia, *Biol Psychiatry* 81(1) (2017) 9-20.
56
57
58
59
60
61
62
63
64
65

- [91] H. Sotoyama, H. Namba, Y. Kobayashi, T. Hasegawa, D. Watanabe, E. Nakatsukasa, K. Sakimura, T. Furuyashiki, H. Nawa, Resting-state dopaminergic cell firing in the ventral tegmental area negatively regulates affiliative social interactions in a developmental animal model of schizophrenia, *Transl Psychiatry* 11(1) (2021) 236.
- [92] M. Kokkinou, E.E. Irvine, D.R. Bonsall, S. Natesan, L.A. Wells, M. Smith, J. Glegola, E.J. Paul, K. Tossell, M. Veronese, S. Khadayate, N. Dedic, S.C. Hopkins, M.A. Ungless, D.J. Withers, O.D. Howes, Reproducing the dopamine pathophysiology of schizophrenia and approaches to ameliorate it: a translational imaging study with ketamine, *Mol Psychiatry* 26(6) (2021) 2562-2576.
- [93] C.S. Peterson, S.L. Baglot, N.A. Sallam, S. Mina, M.N. Hill, S.L. Borgland, Oral pre- and early postnatal cannabis exposure disinhibits ventral tegmental area dopamine neuron activity but does not influence cocaine preference in offspring in mice, *J Neurosci Res* 102(7) (2024) e25369.
- [94] M.H. Sarikahya, S. Cousineau, M. De Felice, K. Lee, K.K. Wong, M.V. DeVuono, T. Jung, M. Rodriguez-Ruiz, T.H.J. Ng, D. Gummerson, E. Proud, D.B. Hardy, K.K. Yeung, W. Rushlow, S.R. Laviolette, Prenatal THC Exposure Induces Sex-Dependent Neuropsychiatric Endophenotypes in Offspring and Long-Term Disruptions in Fatty-Acid Signaling Pathways Directly in the Mesolimbic Circuitry, *eNeuro* 9(5) (2022).
- [95] M. Ironside, P. Kumar, M. Kang, D. Pizzagalli, Brain mechanisms mediating effects of stress on reward sensitivity, *Current Opinion in Behavioral Sciences* 22 (2018) 106-113.
- [96] D. Payer, B. Williams, E. Mansouri, S. Stevanovski, S. Nakajima, B. Le Foll, S. Kish, S. Houle, R. Mizrahi, S.R. George, T.P. George, I. Boileau, Corticotropin-releasing hormone and dopamine release in healthy individuals, *Psychoneuroendocrinology* 76 (2017) 192-196.
- [97] A. Bara, J.N. Ferland, G. Rompala, H. Szutorisz, Y.L. Hurd, Cannabis and synaptic reprogramming of the developing brain, *Nat Rev Neurosci* 22(7) (2021) 423-438.
- [98] R.J. Ellis, A. Bara, C.A. Vargas, A.L. Frick, E. Loh, J. Landry, T.O. Uzamere, J.E. Callens, Q. Martin, P. Rajarajan, K. Brennand, A. Ramakrishnan, L. Shen, H. Szutorisz, Y.L. Hurd, Prenatal Delta(9)-Tetrahydrocannabinol Exposure in Males Leads to Motivational Disturbances Related to Striatal Epigenetic Dysregulation, *Biol Psychiatry* 92(2) (2022) 127-138.
- [99] Y.L. Hurd, J.N. Ferland, Y. Nomura, L.A. Hulvershorn, K.M. Gray, C. Thurstone, Cannabis Use and the Developing Brain: Highs and Lows, *Front Young Minds* 11 (2023).
- [100] Y.L. Hurd, O.J. Manzoni, M.V. Pletnikov, F.S. Lee, S. Bhattacharyya, M. Melis, Cannabis and the Developing Brain: Insights into Its Long-Lasting Effects, *J Neurosci* 39(42) (2019) 8250-8258.
- [101] H. Szutorisz, Y.L. Hurd, High times for cannabis: Epigenetic imprint and its legacy on brain and behavior, *Neurosci Biobehav Rev* 85 (2018) 93-101.
- [102] A. Bara, A. Manduca, A. Bernabeu, M. Borsoi, M. Serviado, O. Lassalle, M.N. Murphy, J. Wager-Miller, K. Mackie, A.L. Pelissier-Alicot, V. Trezza, O.J. Manzoni, Sex-dependent effects of in utero cannabinoid exposure on cortical function, *Elife* 7 (2018).
- [103] T. Black, S.L. Baccetto, I.L. Barnard, E. Finch, D.L. McElroy, F.V.L. Austin-Scott, Q. Greba, D. Michel, A. Zagzoog, J.G. Howland, R.B. Laprairie, Characterization of cannabinoid plasma concentration, maternal health, and cytokine levels in a rat model of prenatal Cannabis smoke exposure, *Sci Rep* 13(1) (2023) 21070.
- [104] E. Murru, G. Carta, C. Manca, M. Verce, A. Everard, V. Serra, S. Aroni, M. Melis, S. Banni, Impact of Prenatal THC Exposure on Lipid Metabolism and Microbiota Composition in Rat Offspring. , *Helyion* (2024).
- [105] A.F. Scheyer, M. Melis, V. Trezza, O.J.J. Manzoni, Consequences of Perinatal Cannabis Exposure, *Trends Neurosci* 42(12) (2019) 871-884.
- [106] G.I. Robinson, F. Ye, X. Lu, S.R. Laviolette, Q. Feng, Maternal Delta-9-Tetrahydrocannabinol Exposure Induces Abnormalities of the Developing Heart in Mice, *Cannabis Cannabinoid Res* 9(1) (2024) 121-133.
- [107] H. Chang, M. Perkins, L. Novaes, F. Qian, T. Zhang, P. Neckel, S. Scherer, R. Ley, W. Han, I. de Araujo, Stress-sensitive neural circuits change the gut microbiome via duodenal glands, *Cell* (2024).
- [108] E.R. de Kloet, M.L. Molendijk, Floating Rodents and Stress-Coping Neurobiology, *Biol Psychiatry* 90(4) (2021) e19-e21.
- [109] J.E. Sutherland, L.C. Burian, J. Covault, L.H. Conti, The effect of restraint stress on prepulse inhibition and on corticotropin-releasing factor (CRF) and CRF receptor gene expression in Wistar-Kyoto and Brown Norway rats, *Pharmacol Biochem Behav* 97(2) (2010) 227-38.

- 1 [110] Y. Oda, N. Kanahara, H. Kimura, H. Watanabe, K. Hashimoto, M. Iyo, Genetic association
2 between G protein-coupled receptor kinase 6/beta-arrestin 2 and dopamine supersensitivity
3 psychosis in schizophrenia, *Neuropsychiatr Dis Treat* 11 (2015) 1845-51.
- 4 [111] M. Tamura, J. Mukai, J.A. Gordon, J.A. Gogos, Developmental Inhibition of Gsk3 Rescues
5 Behavioral and Neurophysiological Deficits in a Mouse Model of Schizophrenia Predisposition,
6 *Neuron* 89(5) (2016) 1100-9.
- 7 [112] L. Stertz, J. Di Re, G. Pei, G.R. Fries, E. Mendez, S. Li, L. Smith-Callahan, H. Raventos, J.
8 Tipo, R. Cherukuru, Z. Zhao, Y. Liu, P. Jia, F. Laezza, C. Walss-Bass, Convergent genomic and
9 pharmacological evidence of PI3K/GSK3 signaling alterations in neurons from schizophrenia
10 patients, *Neuropsychopharmacology* 46(3) (2021) 673-682.
- 11 [113] S. Matsuda, Y. Ikeda, M. Murakami, Y. Nakagawa, A. Tsuji, Y. Kitagishi, Roles of
12 PI3K/AKT/GSK3 Pathway Involved in Psychiatric Illnesses, *Diseases* 7(1) (2019).
- 13 [114] P. Wong, C.C. Chang, C.E. Marx, M.G. Caron, W.C. Wetsel, X. Zhang, Pregnenolone
14 rescues schizophrenia-like behavior in dopamine transporter knockout mice, *PLoS One* 7(12)
15 (2012) e51455.
- 16 [115] E.M. Hur, F.Q. Zhou, GSK3 signalling in neural development, *Nat Rev Neurosci* 11(8) (2010)
17 539-51.
- 18 [116] J.M. Beaulieu, A role for Akt and glycogen synthase kinase-3 as integrators of dopamine and
19 serotonin neurotransmission in mental health, *J Psychiatry Neurosci* 37(1) (2012) 7-16.
- 20 [117] C.S. Karam, J.S. Ballon, N.M. Bivens, Z. Freyberg, R.R. Girgis, J.E. Lizardi-Ortiz, S. Markx,
21 J.A. Lieberman, J.A. Javitch, Signaling pathways in schizophrenia: emerging targets and
22 therapeutic strategies, *Trends Pharmacol Sci* 31(8) (2010) 381-90.
- 23 [118] P. Su, H. Zhang, A.H.C. Wong, F. Liu, The DISC1 R264Q variant increases affinity for the
24 dopamine D2 receptor and increases GSK3 activity, *Mol Brain* 13(1) (2020) 87.
- 25 [119] Z. Freyberg, S.J. Ferrando, J.A. Javitch, Roles of the Akt/GSK-3 and Wnt signaling pathways
26 in schizophrenia and antipsychotic drug action, *Am J Psychiatry* 167(4) (2010) 388-96.
- 27 [120] D.Z. Luo, C.Y. Chang, T.R. Huang, V. Studer, T.W. Wang, W.S. Lai, Lithium for schizophrenia:
28 supporting evidence from a 12-year, nationwide health insurance database and from Akt1-deficient
29 mouse and cellular models, *Sci Rep* 10(1) (2020) 647.
- 30 [121] P. Duda, J. Wisniewski, T. Wojtowicz, O. Wojcicka, M. Jaskiewicz, D. Drulis-Fajdasz, D.
31 Rakus, J.A. McCubrey, A. Gizak, Targeting GSK3 signaling as a potential therapy of
32 neurodegenerative diseases and aging, *Expert Opin Ther Targets* 22(10) (2018) 833-848.
- 33
34
35
36
37
38
39
40
41
42
43
44
45
46
47
48
49
50
51
52
53
54
55
56
57
58
59
60
61
62
63
64
65

The authors declare that there are not wester blotting data

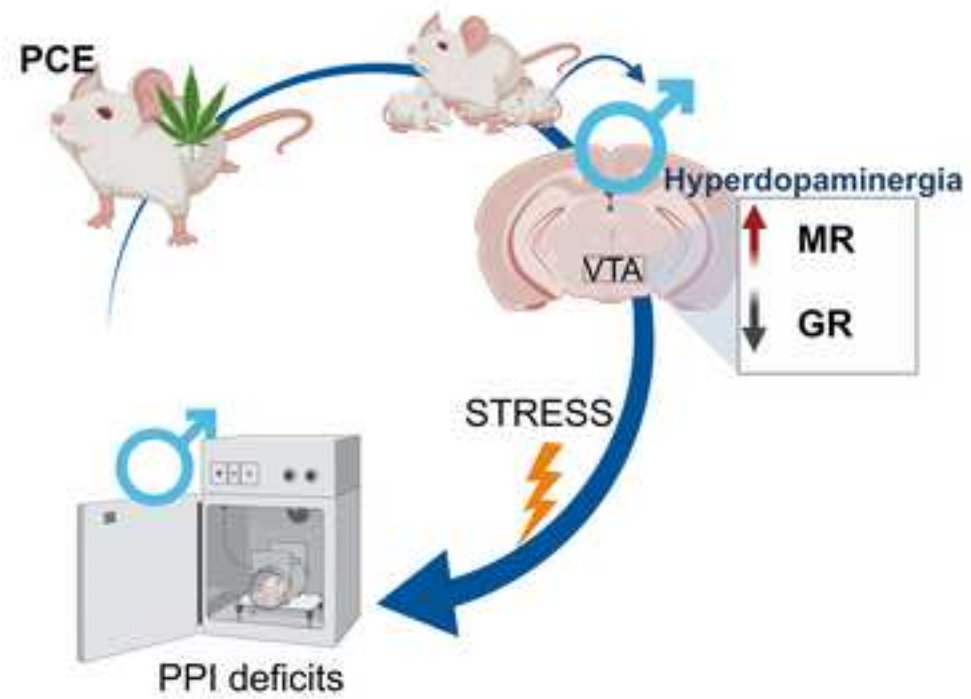
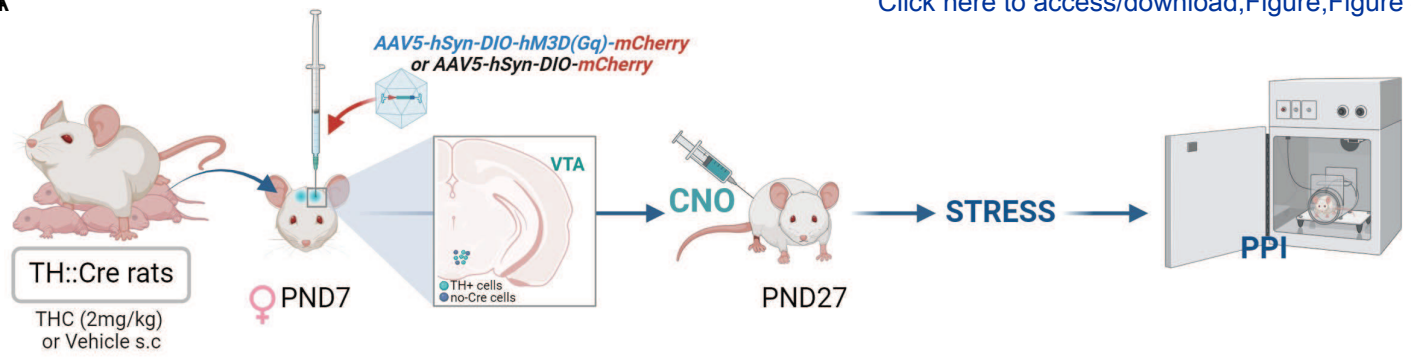
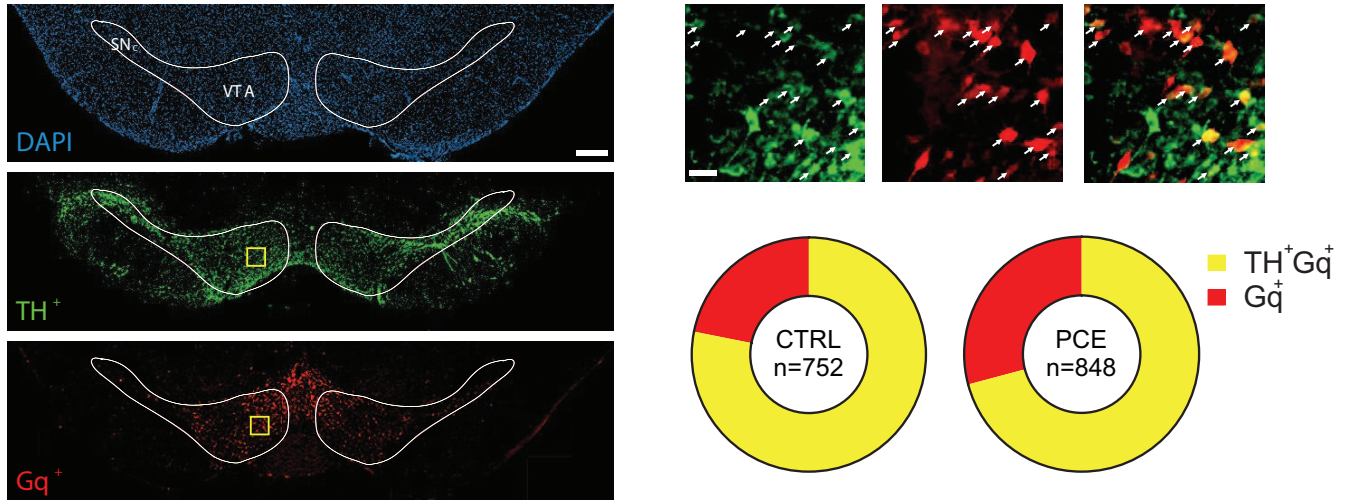


Figure A

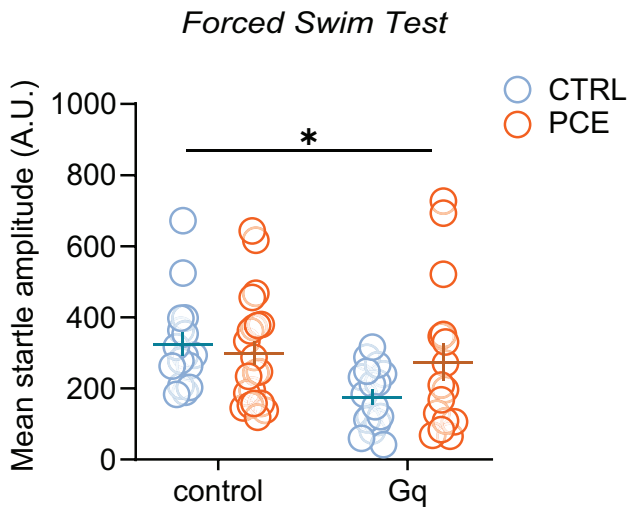
[Click here to access/download;Figure;Figure 4.eps](#)



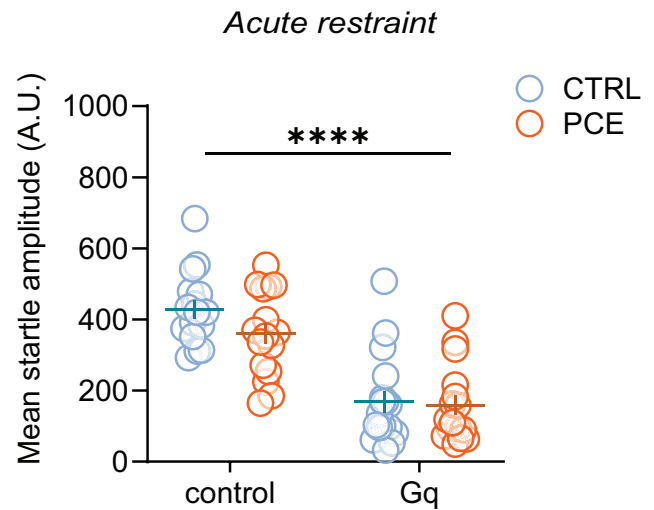
B



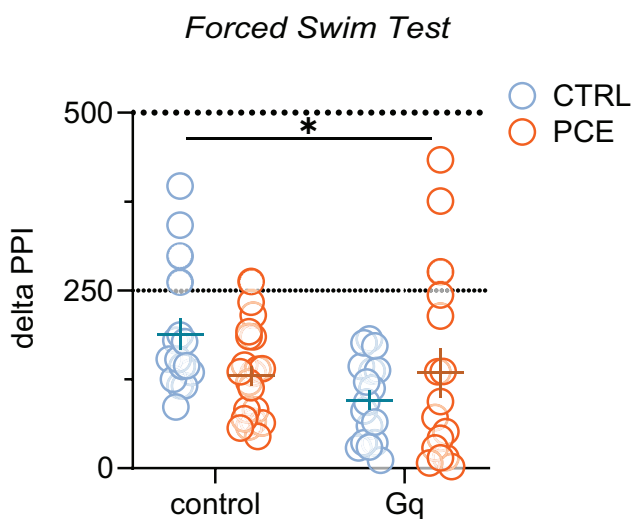
C



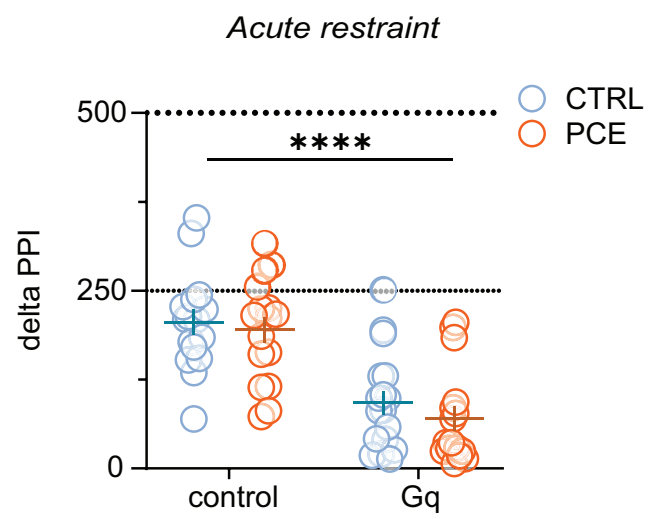
D



E



F



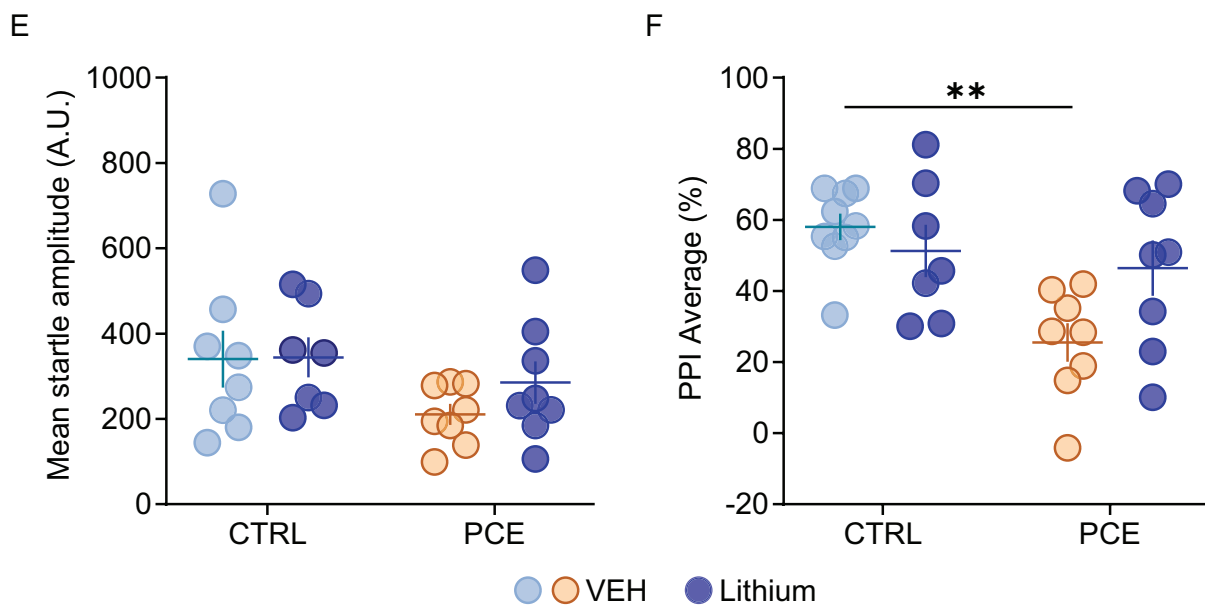
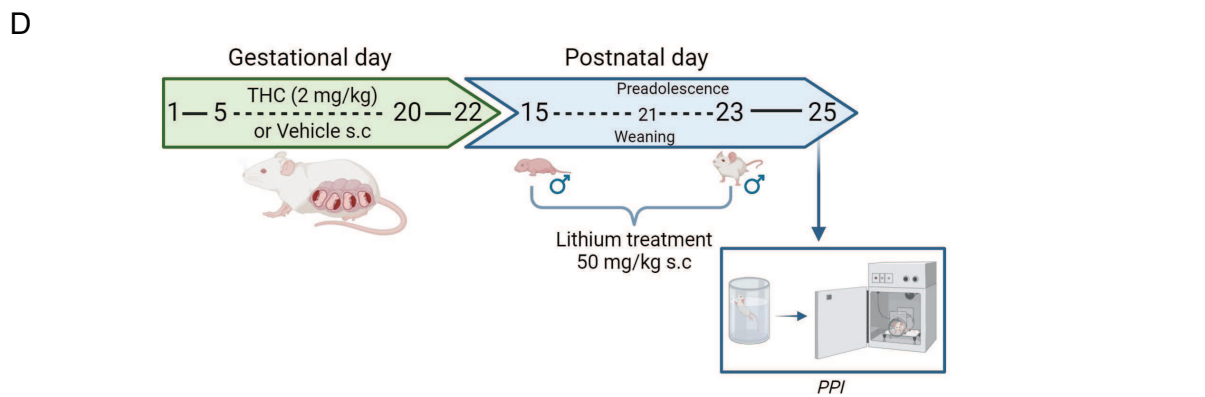
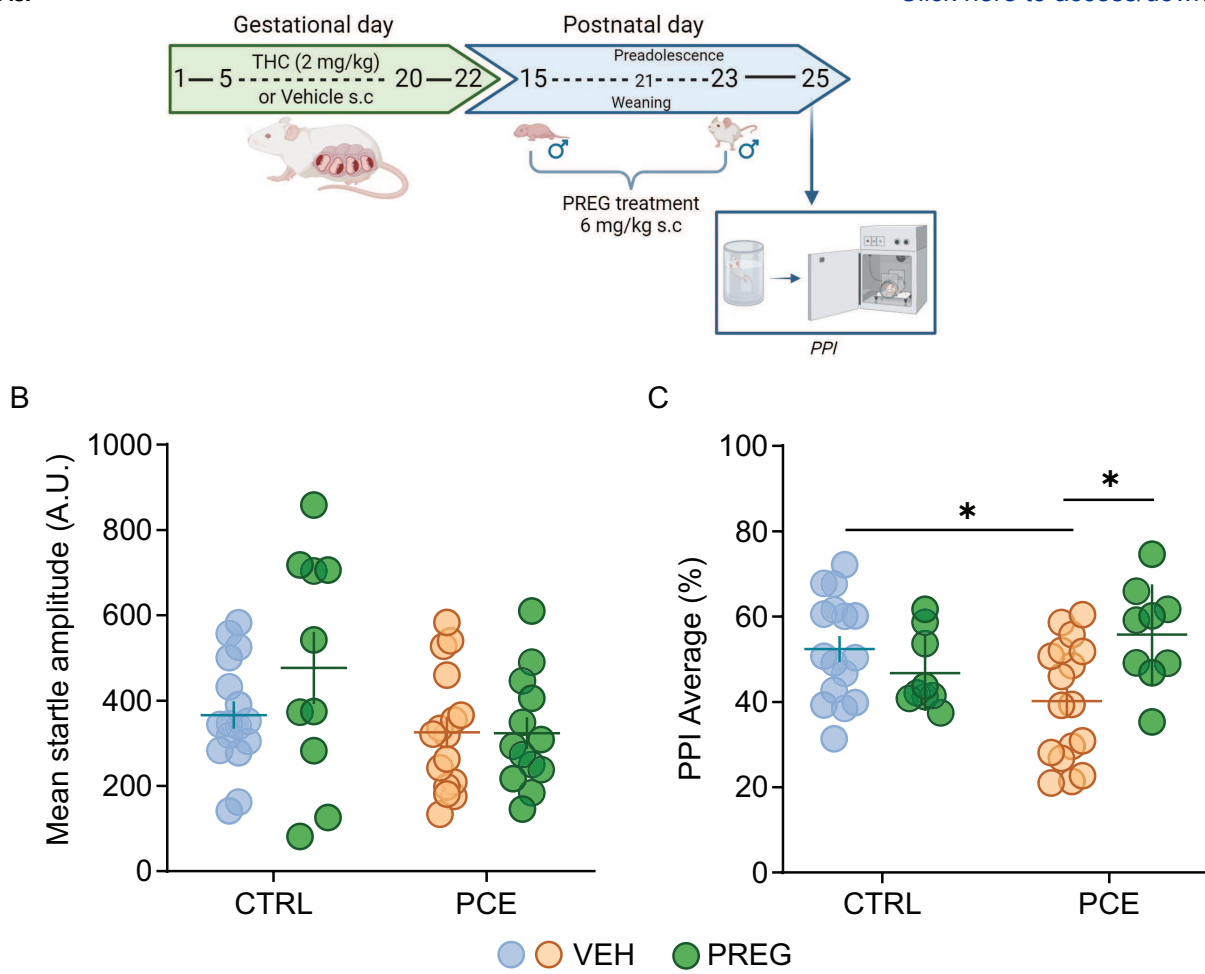
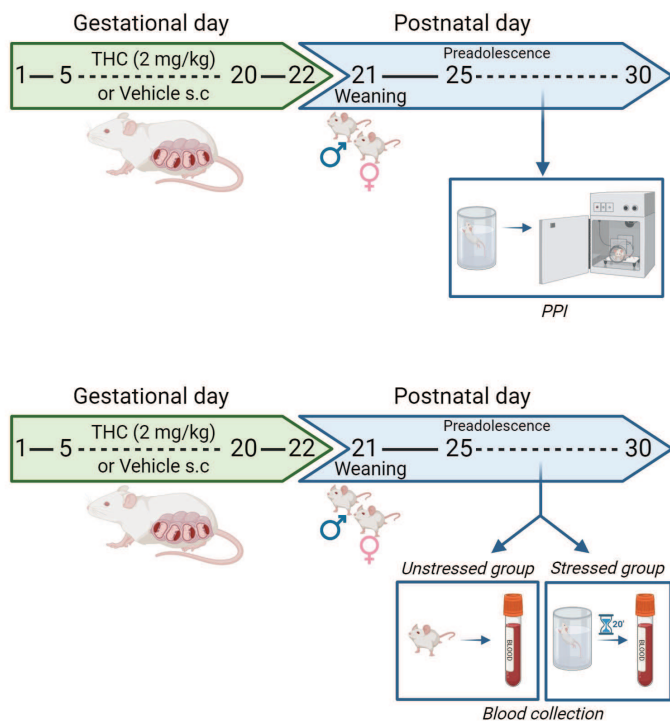
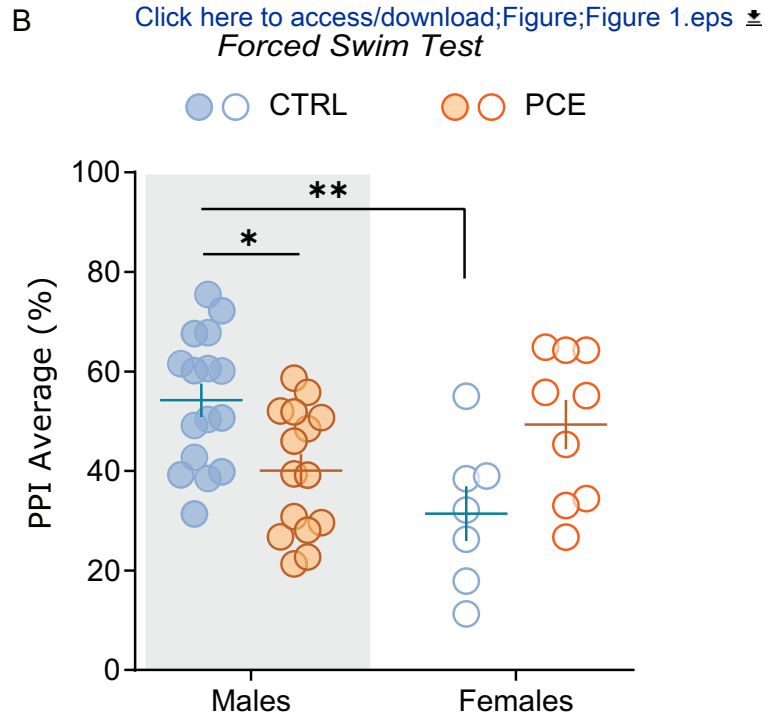


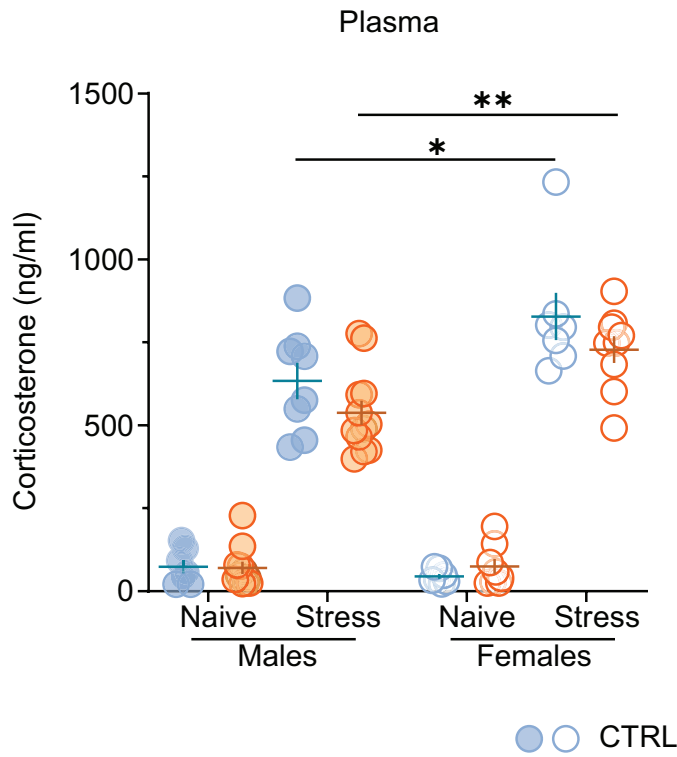
Figure 1A



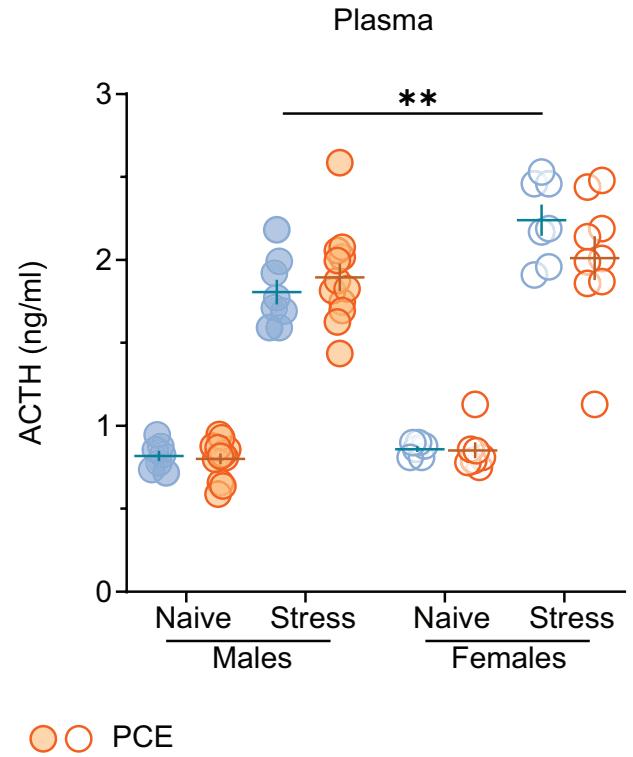
Click here to access/download;Figure;Figure 1.eps

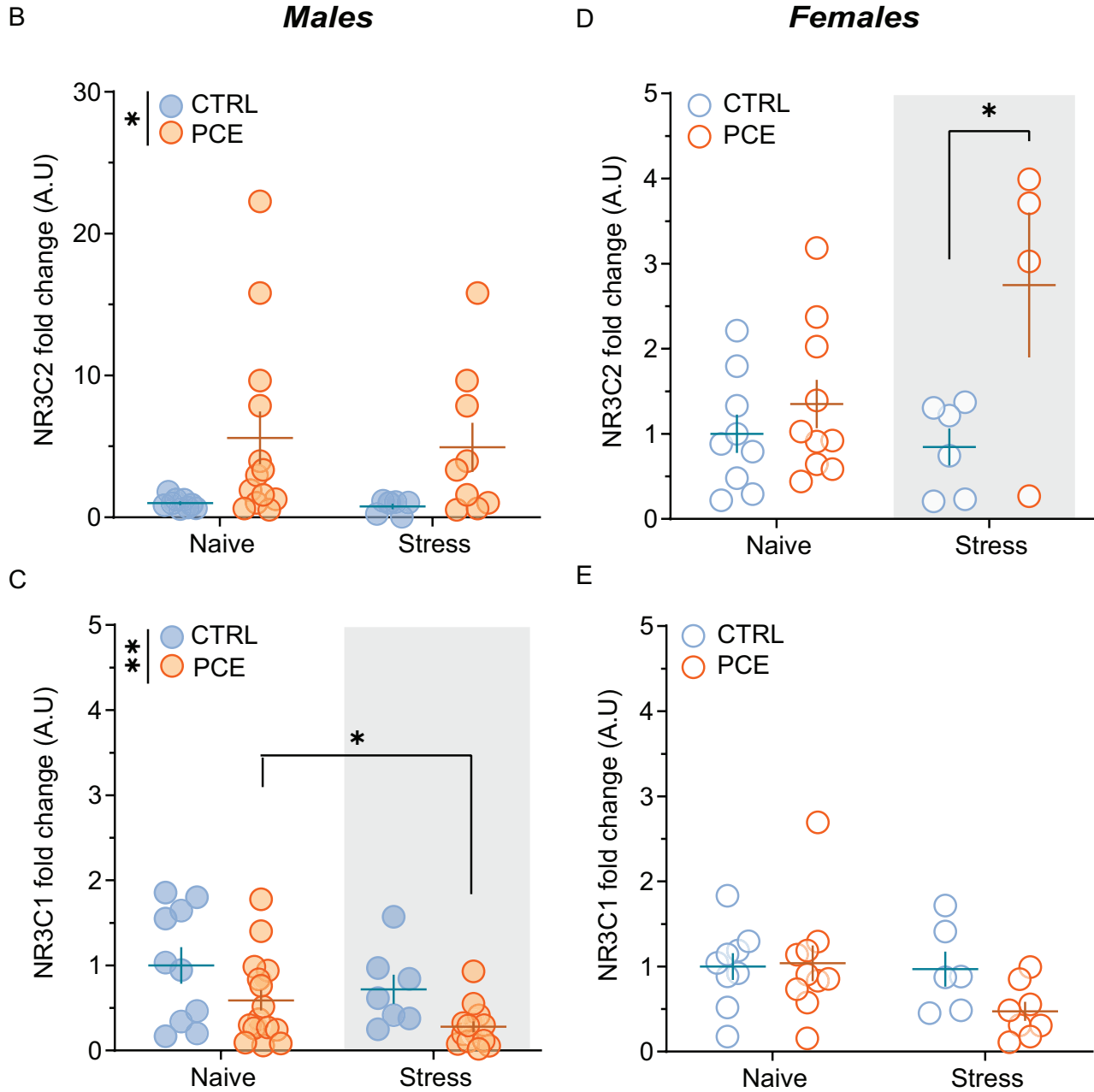
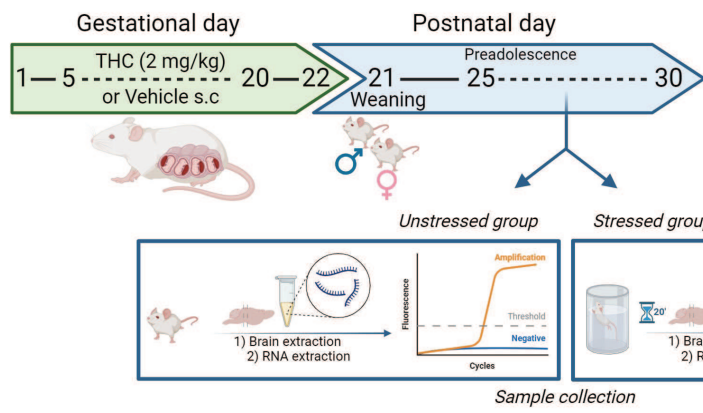


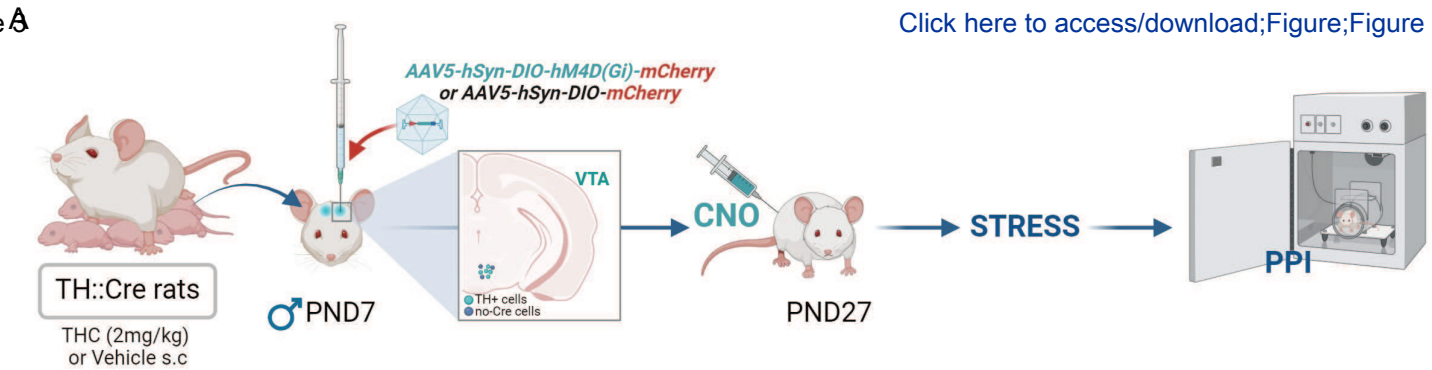
C



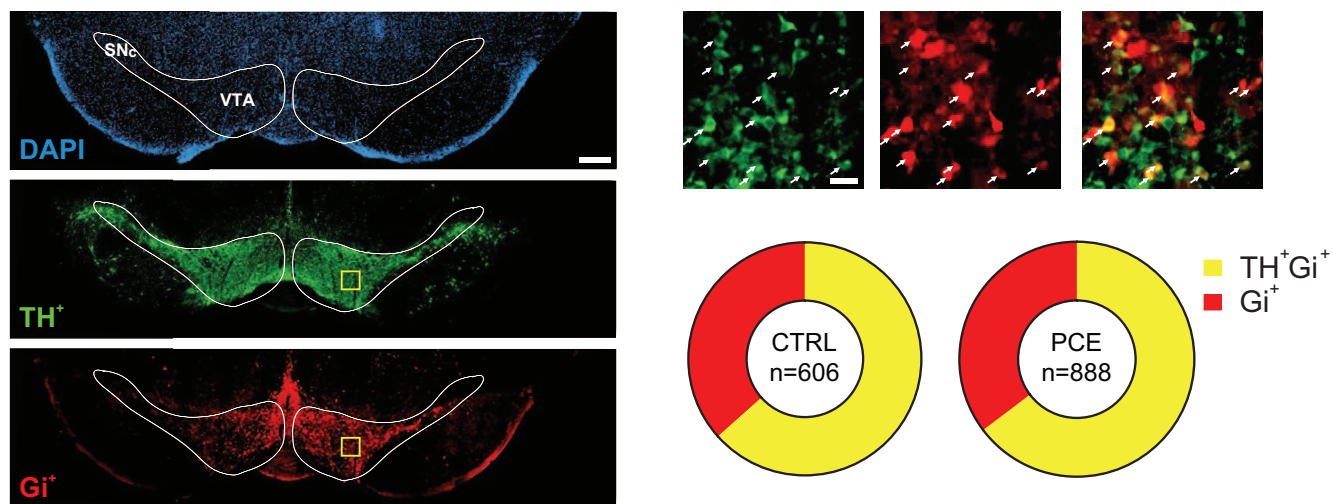
D



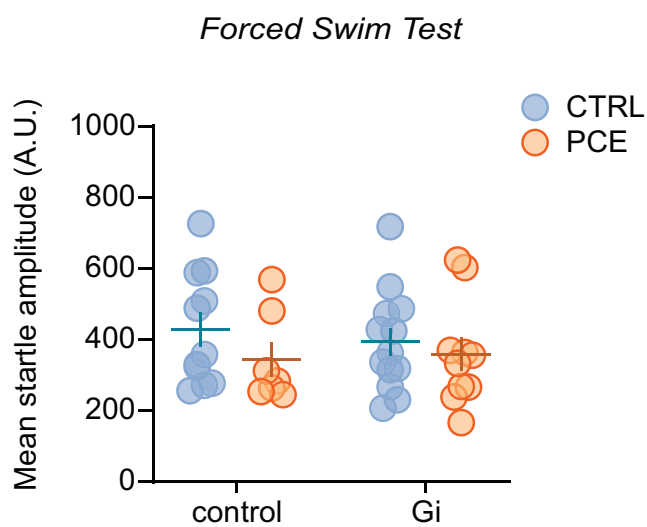




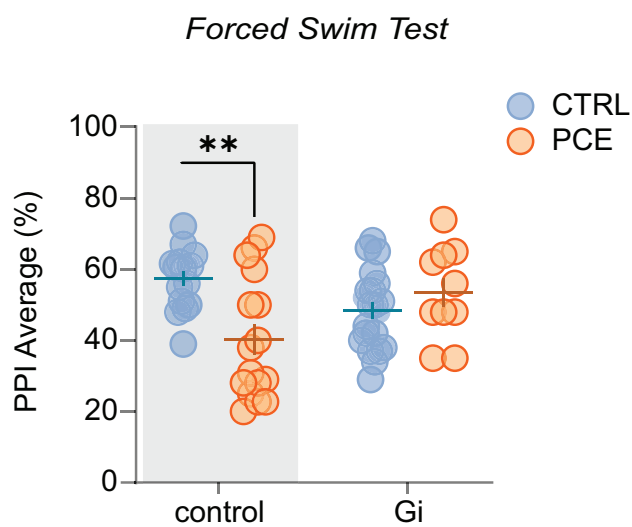
B



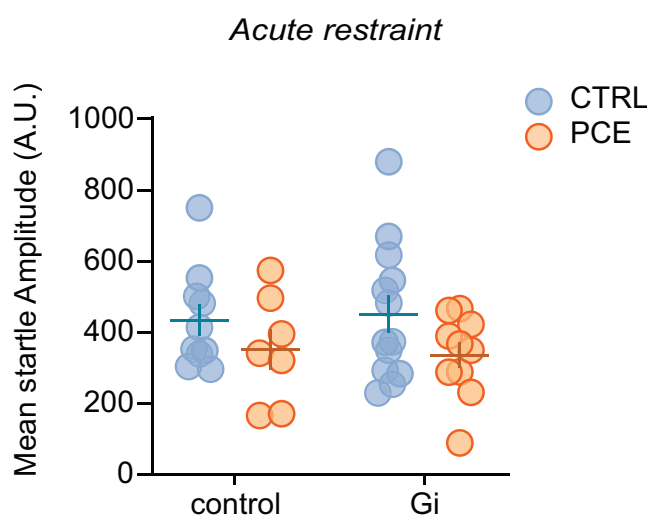
C



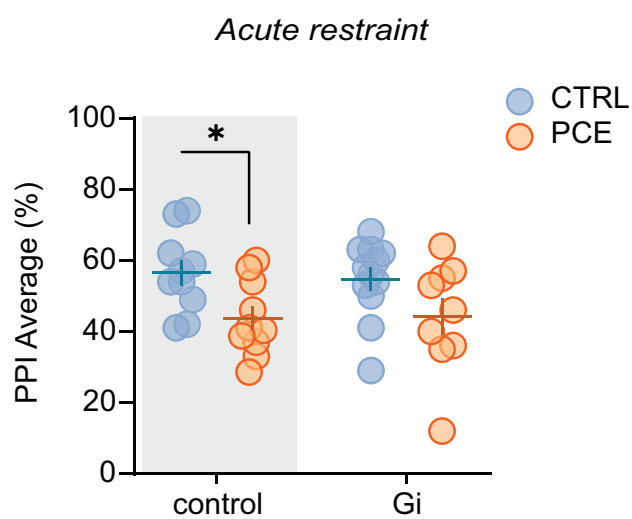
D



E



F



The authors also declare no competing personal or financial interests.